Neuroscience Letters 582 (2014) 120–124

Contents lists available at ScienceDirect

Neuroscience Letters

journal homepage: www.elsevier.com/locate/neulet

Dysbindin-1, a schizophrenia-related protein, interacts with HDAC3

Mika Soma, Min Wang, Satoshi Suo, Shoichi Ishiura*

Department of Life Sciences, Graduate School of Arts and Sciences, The University of Tokyo, 3-8-1 Komaba, Meguro-ku, Tokyo 153-8902, Japan

HIGHLIGHTS

- Dysbindin-1 interacts with HDAC3 *in vivo*.
- Dysbindin-1A and -1B interact with HDAC3 but -1C does not.
- Dysbindin-1B expression is increased in the nucleus in the presence of HDAC3.
- The phosphorylation level of HDAC3 increased in the presence of dysbindin-1B.

ARTICLE INFO

Article history:
Received 2 May 2014
Received in revised form 13 August 2014
Accepted 26 August 2014
Available online 6 September 2014

Keywords:
Schizophrenia
Dysbindin-1
HDAC3
Interaction
Isoform
Phosphorylation

ABSTRACT

DTNBP1 is a key candidate gene associated with schizophrenia. The expression of its protein product, dysbindin-1, is altered in the brains of schizophrenic patients; however, the physiological functions of dysbindin-1 in the central nervous system are unclear. Several studies have shown that both dysbindin-1 and histone deacetylase 3 (HDAC3) can be phosphorylated by the DNA-dependent protein kinase complex. In this study, we investigated the relationship between dysbindin-1 and HDAC3. We found that dysbindin-1 formed a protein complex with HDAC3 in human neuroblastoma cells and in mouse brain. The interaction between dysbindin-1 and HDAC3 occurred in an isoform-specific manner: HDAC3 coupled with dysbindin-1A and -1B, but not -1C. We also found that dysbindin-1B expression was increased in the nucleus in the presence of HDAC3, and, conversely, that the phosphorylation level of HDAC3 increased in the presence of dysbindin-1B. Taken together, these results identify a novel binding partner for dysbindin-1, which may potentially provide a new avenue for research into the neurological mechanisms of schizophrenia.

1. Introduction

Schizophrenia is a chronic mental disorder characterized by positive symptoms such as hallucinations and delusions, and negative symptoms such as dullness of thinking and behavior, as well as cognitive disorders in memory and learning. Numerous studies have suggested that genetic factors contribute to schizophrenia, and several genes, including *DISC1*, *NRG1*, and *DTNBP1*, have been identified as schizophrenia susceptibility genes [14,19,20]. *DTNBP1* is situated at chromosomal locus 6p22.3, a location with established linkage to schizophrenia [17,21,28]. *DTNBP1* has several SNPs that are suggested to influence the risk of developing schizophrenia [18,20]. Since the SNPs in *DTNBP1* are in an intron, and not in an exon, they do not affect the amino acid sequence of the encoded protein, dysbindin-1; rather, they regulate the expression of dysbindin-1 mRNA and protein [2]. Recent postmortem brain studies have shown that the expression of dysbindin-1 mRNA and protein is reduced in the brains of schizophrenic patients [24,25,29,30]. Furthermore, it has been reported that dysbindin-1-deficient mice are less active and display reduced novelty-seeking behavior, similar to the negative symptoms of schizophrenia, and that they show cognitive deficiencies in learning and memory [1,3,5,7,9,23]. Therefore, it is thought that dysbindin-1 expression is reduced in schizophrenic patients, preventing the protein from fulfilling its normal physiological function and contributing to the symptoms of schizophrenia.

Although most studies have addressed the function of dysbindin-1 in the cytoplasm, dysbindin-1 is also found in the nucleus [16]. It has been reported that dysbindin-1 interacts with nuclear proteins such as nuclear transcription factor Y beta (NF-YB) and the DNA-dependent protein kinase (DNA-PK) complex [15,16]. Dysbindin-1 interacts with and is phosphorylated by the DNA-PK complex [16]. The DNA-PK complex also interacts with and phosphorylates histone deacetylase 3 (HDAC3), which is a transcriptional regulator [11]. HDAC3 is particular in Class I HDACs, because HDAC3 is able to shuttle between the cytoplasm and

* Corresponding author. Tel.: +81 3 5454 6739; fax: +81 3 5454 6739.
E-mail address: cishiura@mail.ecc.u-tokyo.ac.jp (S. Ishiura).

http://dx.doi.org/10.1016/j.neulet.2014.08.046
0304-3940/

the nucleus in certain conditions [22,31]. The knockout of HDAC3 in mouse hippocampus enhances long-term memory, suggesting that HDAC3 is a negative regulator of long-term memory formation [12]. In addition, HDAC inhibitors are expected to be effective drugs for the treatment of psychiatric disorders, including schizophrenia, based on evidence showing that histone acetylation is reduced in patients with psychiatric disorders [4,8,27]. Because both dysbindin-1 and HDAC3 are phosphorylated by the DNA-PK complex, we sought to investigate the relationship between these two proteins. The proposed overlap in function and subcellular distribution profiles between dysbindin-1 and HDAC3 strongly suggest a specific interaction; however, this hypothesis has not yet been directly tested.

In this study, we show that dysbindin-1 isoforms A and B, but not C, interact with HDAC3. In addition, the expression of dysbindin-1B increases in the nucleus in the presence of HDAC3, and it facilitates the phosphorylation of HDAC3.

2. Materials and methods

2.1. Antibodies

Rabbit polyclonal antibodies against dysbindin-1 were generated according to the previous report [16].

Anti-V5 and -lamin B mouse monoclonal antibodies were purchased from Life Technologies (Carlsbad, CA). The following rabbit polyclonal antibodies were purchased from the indicated vendors: anti-HDAC3 (Abcam, Cambridge, UK), anti-phospho-HDAC3, anti-myc, and anti-α-tubulin (all Cell Signaling Technology, Inc., Beverly, MA). Anti-GST goat polyclonal antibodies were purchased from GE Healthcare (Cleveland, OH).

2.2. Plasmid construction

The cDNAs encoding HDAC3 and the three isoforms of human dysbindin-1 were cloned from a human fetal brain cDNA library (BD Biosciences, San Jose, CA) by polymerase chain reaction. The cDNAs were subcloned into pcDNA3.1 (Invitrogen, Carlsbad, CA) or pGEX-5X-1 (GE Healthcare), which contain a hexahistidine tag at the C-terminus. Myc-dysbindin-1 contained six myc tags at the N-terminus of dysbindin-1. GST-dysbindin-1 contained a GST tag at the N-terminus and three His tags the C-terminus of dysbindin-1. V5-HDAC3 contained a V5 tag at the C-terminus of HDAC3. All constructs were confirmed by sequencing [16].

2.3. Expression and purification of GST and GST-dysbindin-1 and GST pull-down assay

GST and GST-dysbindin-1 were purified and GST pull-down assay was performed according to the previous report [16].

2.4. Co-immunoprecipitation

Lysates (800 μg per sample) diluted in 500 μL of NP-40 buffer were precleared with 30 μL of Protein G Sepharose 4 Fast Flow beads (GE Healthcare) for 2 h at 4 °C. The precleared lysates and antibodies linked to Protein G Sepharose 4 Fast Flow beads were incubated for 4 h at 4 °C. After washing, sample buffer was added, and the samples were boiled for 5 min at 100 °C. The precipitates were analyzed by SDS-PAGE and immunoblotting.

2.5. Subcellular fractionation

Subcellular fractionation was performed with a Qproteome Cell Compartment Kit (Qiagen) according to the manufacturer's protocol.

2.6. HDAC3 phosphorylation level analysis

Immunoprecipitation was performed using 500 μL of a lysate prepared from HEK293 cells expressing myc-dysbindin-1 and V5-HDAC3, and anti-V5 antibody-linked Protein G Sepharose 4 Fast Flow beads. After washing, the precipitates were divided into two aliquots. To both aliquots, 30 μL of CIAP buffer (50 mM Tris–HCl [pH 9.0], 100 mM NaCl, and 1 mM $MgCl_2$) were added. To one aliquot, 1 μL of calf intestinal alkaline phosphatase (Takara Bio Inc., Otsu, Japan) was also added. The precipitates ware incubated overnight at 37 °C. The precipitates were analyzed by SDS-PAGE and immunoblotting.

2.7. Immunoblotting

Samples were separated by SDS-PAGE and transferred to nitrocellulose membranes (Protran; Whatman, GE Healthcare). The membranes were blocked with 5% skim milk in TBST (100 mM Tris–HCl [pH 7.5], 150 mM NaCl, and 0.05% Tween 20) for 1 h at room temperature and then incubated overnight at 4 °C with primary antibodies in 5% skim milk. After washing, the membranes were incubated for 1 h with horseradish peroxidase-conjugated secondary antibodies at room temperature. The secondary antibodies were purchased from the indicated vendors: anti-rabbit and -mouse IgG (Cell Signaling Technology, Inc.) and anti-goat IgG (Santa Cruz Biotechnology). Immunoreactive bands were visualized by enhanced chemiluminescence (GE Healthcare) and scanned using an LAS 3000 scanner (Fujifilm Co. Ltd., Tokyo, Japan).

3. Results

3.1. Endogenous dysbindin-1 interacts with endogenous HDAC3

To provide evidence for the existence of a dysbindin-1-HDAC3 complex, we first examined whether dysbindin-1 could be co-immunoprecipitated with HDAC3. As shown in Fig. 1A and B, extracts of human neuroblastoma SH-SY5Y cells were subjected to immunoprecipitation with anti-HDAC3 or anti-dysbindin-1 antibodies and an IgG control, followed by immunoblotting for endogenous dysbindin-1 or HDAC3, respectively. Co-immunoprecipitation also demonstrated an interaction between dysbindin-1 and HDAC3 in solubilized mouse forebrain (Fig. 1C). These results suggest that dysbindin-1 interacts with HDAC3 *in vivo*.

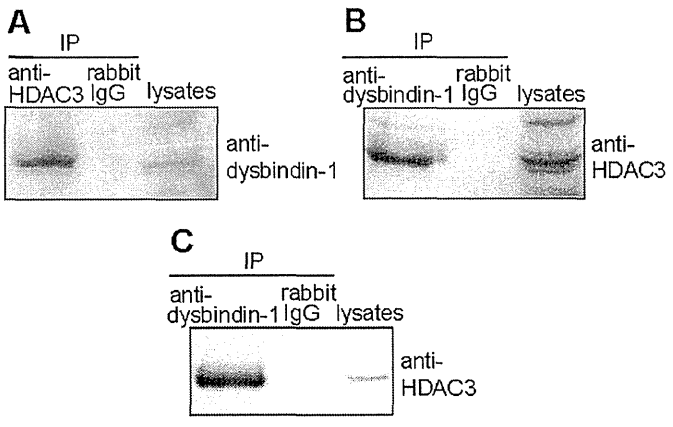

Fig. 1. Interaction between endogenous dysbindin-1 and HDAC3. (A) Co-immunoprecipitation of dysbindin-1 using anti-HDAC3 antibodies in SH-SY5Y cells. (B) Co-immunoprecipitation of HDAC3 using anti-dysbindin-1 antibodies in SH-SY5Y cells. (C) Co-immunoprecipitation of HDAC3 using anti-dysbindin-1 antibodies in mouse forebrain. IP, immunoprecipitation.

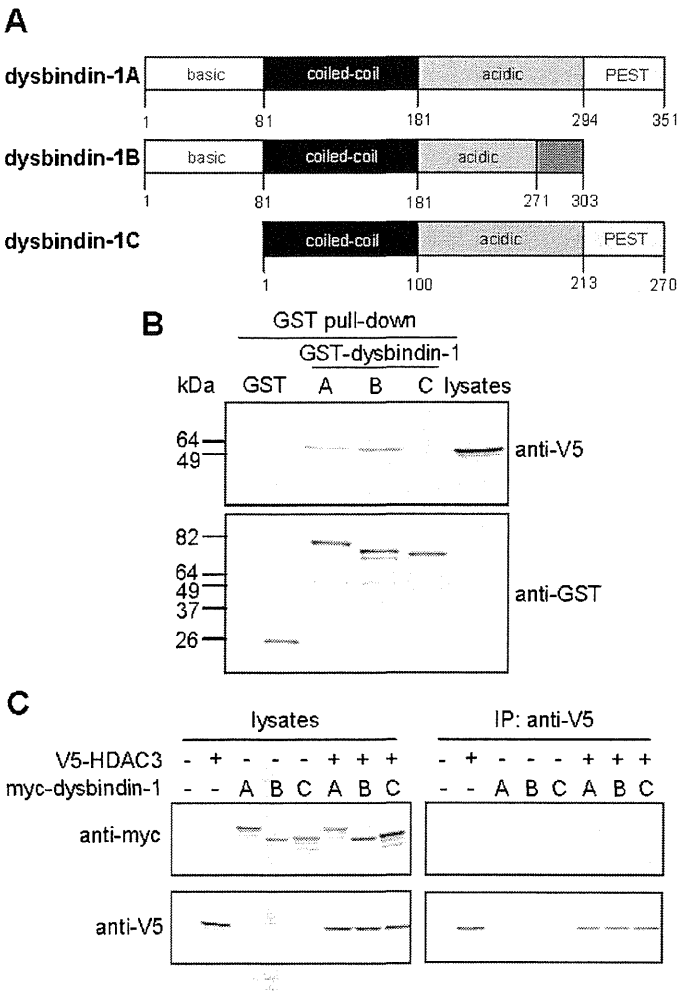

Fig. 2. Identification of the dysbindin-1 isoforms involved in the interaction with HDAC3. (A) Schematic representation of dysbindin-1 isoforms. (B) Western blotting for V5-HDAC3 after affinity precipitation with GST-dysbindin-1 or GST alone, using lysates of HEK293 cells transfected with V5-HDAC3 (upper panel). GST was used as a control (lower panel). (C) Co-immunoprecipitation of myc-dysbindin-1 using anti-V5 antibodies with lysates of HEK293 cells co-transfected with myc-dysbindin-1 and V5-HDAC3. The lysates (left panel) and immunoprecipitates (right panel) are shown. Myc-dysbindin-1 (upper panel) and V5-HDAC3 (lower panel) were detected.

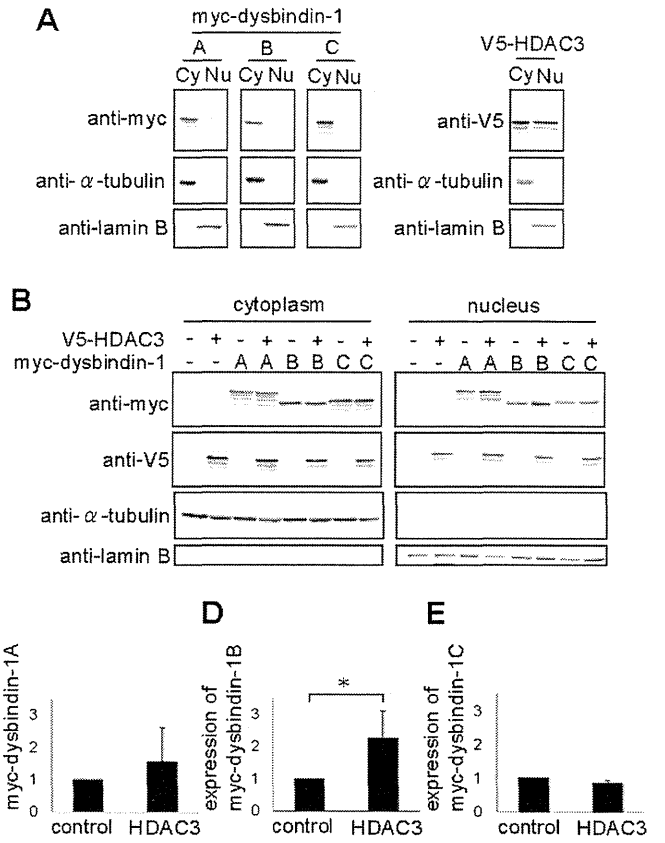

Fig. 3. Subcellular distribution and change in the localization of dysbindin-1 and HDAC3. (A) Subcellular distribution of dysbindin-1 and HDAC3. α-Tubulin and lamin B1 were used as cytoplasmic and nuclear markers, respectively. Cy: cytoplasmic fraction; Nu: nuclear fraction. (B) Change in dysbindin-1 and HDAC3 localization in the presence or absence of each other. (C–E) Quantitation of the nuclear expression of dysbindin-1A (C), -1B (D) and -1C (E). The signal intensity of dysbindin-1 was standardized to the corresponding protein band of lamin B1. The value of the control was designated as 1. *Significantly different from the control group (*$P < 0.05$, $n = 5$); Student's *t*-test.

3.2. Dysbindin-1 interacts with HDAC3 in an isoform-specific manner

Among the proteins of the dysbindin family, dysbindin-1 is the only one that is reportedly associated with schizophrenia. *DTNBP1*, the gene encoding dysbindin-1, has three major transcript isoforms (Fig. 2A) in humans of approximately 50, 37, and 33 kDa, denoted dysbindin-1A, -1B, and -1C, respectively [26]. Expression of these isoforms differs in terms of region, subcellular localization, and developmental time-course [10,25]. To identify the isoform(s) of dysbindin-1 that interact with HDAC3, we constructed GST fusion proteins encoding the A to C isoforms of human dysbindin-1. Affinity pull-down assays of proteins from lysates of HEK293 cells transfected with V5-HDAC3 were performed, with GST alone as a control. As shown in Fig. 2B, dysbindin-1A and -1B, but not -1C or GST alone, precipitated V5-HDAC3, indicating that dysbindin-1 interacts with HDAC3 in an isoform-specific manner. To further confirm this isoform-specific interaction, we also performed co-immunoprecipitation using HEK293 cells co-transfected with myc-tagged dysbindin-1 (isoforms A–C) and V5-HDAC3. As illustrated in Fig. 2C, myc-tagged dysbindin-1A and -1B, but not -1C, co-immunoprecipitated with V5-HDAC3, in agreement with our affinity pull-down results. Taken together, these data indicate that dysbindin-1 interacts with HDAC3 in an isoform-specific manner.

3.3. Formation of the dysbindin-1-HDAC3 complex influences the subcellular distribution of dysbindin-1B

Previous studies demonstrated that endogenous dysbindin-1 localizes mainly to the cytoplasm, with some diffuse expression in the nucleus [6,16,], while HDAC3, is able to shuttle between the cytoplasm and the nucleus in certain conditions [22,31]. This overlapping subcellular distribution suggests that the dysbindin-1-HDAC3 complex regulates the localization of dysbindin-1 and/or HDAC3. To confirm the subcellular distribution of dysbindin-1 and HDAC3 in our system, we performed subcellular fractionation of HEK293 cells transfected with myc-dysbindin-1 (isoforms A–C) or V5-HDAC3, followed by immunoblotting. Lamin B1 and α-tubulin were used as nuclear and cytosolic markers, respectively. Dysbindin-1 (isoforms A–C) was localized primarily in the cytoplasmic fraction, with a small amount in the nuclear fraction (Fig. 3A). Next to study the effect of the dysbindin-1-HDAC3 complex, we co-transfected HEK293 cells with myc-dysbindin-1 (isoforms A–C) and V5-HDAC3. As shown in Fig. 3B, both dysbindin-1A and -1B exhibited increased nuclear localization in the presence of HDAC3; however, only the increase in dysbindin-1B was statistically significant (Fig. 3D). A localization change for HDAC3 was not observed in either the nuclear or cytoplasmic fraction (Fig. 3B). Taken together,

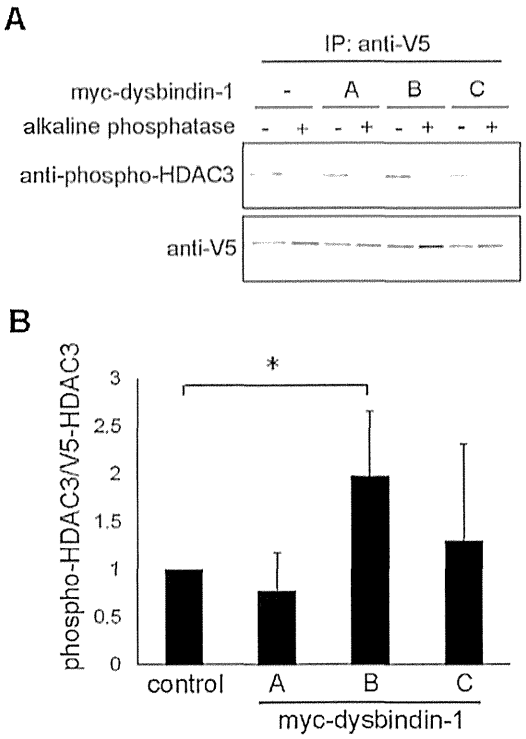

Fig. 4. The HDAC3 phosphorylation level is altered in the presence of dysbindin-1. (A) Western blotting for phospho-HDAC3 and V5-HDAC3 in the presence of dysbindin-1. (B) Quantitation of phospho-HDAC3 in the presence of dysbindin-1. The signal intensity of phospho-HDAC3 was standardized to the corresponding protein band of V5-HDAC3. The value of the control was designated as 1.*Significantly different from the control group (*$P < 0.05$, $n = 6$); Dunnett's test.

these results suggest that dysbindin-1B translocates to the nucleus in the presence of HDAC3.

3.4. Dysbindin-1B promotes HDAC3 phosphorylation

We next investigated the functional significance of dysbindin-1-HDAC3 complex formation. Because dysbindin-1 and HDAC3 are reported to be phosphorylated by the same DNA-PK complex [11,16], we assessed the influence of the dysbindin-1-HDAC3 complex on HDAC3 phosphorylation in HEK293 cells co-transfected with myc-dysbindin-1 (isoforms A–C) and V5-HDAC3. HDAC3 was immunoprecipitated using anti-V5 antibodies, and HDAC3 phosphorylation was detected using anti-phospho-HDAC3 (Ser424) antibodies. As a negative control, immunoprecipitation was carried out side-by-side in the presence of alkaline phosphatase to confirm the specificity of the phosphorylation antibody. As shown in Fig. 4A, the phosphorylation of HDAC3 at Ser424 was significantly increased by almost two-fold when dysbindin-1B, but not -1A or -1C, was co-transfected. The phospho-HDAC3 band intensities were quantified and normalized to the expression level of HDAC3, as shown in Fig. 4B. These data suggest that the interaction between dysbindin-1B and HDAC3 regulates HDAC3 phosphorylation.

4. Discussion

In this study, we demonstrated an interaction between dysbindin-1 and HDAC3 *in vivo*, in both human neuroblastoma cells and mouse brain tissue. In addition, we showed by GST pull-down and co-immunoprecipitation assays that dysbindin-1A and -1B, but not -1C, interact with HDAC3. This isoform-specific interaction may be attributable to the differences in amino acid sequence of the spliced isoforms of dysbindin-1. As shown in Fig. 2A, dysbindin-1A is the full-length form while -1B has a different, shorter C-terminus from -1A, and -1C lacks the N-terminus of -1A. Based on our results, the domain of dysbindin-1 required for the interaction with HDAC3 is likely to be in the N-terminus and common to -1A and -1B. Future studies are required to delineate the specific region(s) involved in this interaction.

Previous reports have shown that dysbindin-1 is expressed in the nuclei of hippocampal neurons *in vivo* [24], and that dysbindin-1 has a functional nuclear export signal facilitating nucleocytoplasmic shuttling of dysbindin-1, which affects its regulation of synapsin I expression [6]. However, the precise function of dysbindin-1 in the nucleus remains largely unknown. Therefore, we examined whether the dysbindin-1-HDAC3 complex affects the subcellular localization of dysbindin-1 (A–C) or HDAC3. Surprisingly, although both dysbindin-1A and -1B bound HDAC3, only dysbindin-1B exhibited a significant increase in nuclear localization in the presence of HDAC3, as demonstrated by subcellular fractionation. Although Oyama et al. [16] reported that dysbindin-1 bound DNA-PK in an isoform-dependent manner, functional differences among these three isoforms remain unclear. Future studies are required to investigate whether this is due to the difference in amino acid sequence between dysbindin-1A and -1B or other factors (*e.g.*, subcellular distribution). Previous reports have also shown that dysbindin-1 can be exported from the nucleus to the cytoplasm by exportin-1/CRM1-mediated nuclear export. Furthermore, nuclear dysbindin-1 transcriptionally regulates synapsin I gene expression [6]. Therefore, it is possible that in our system the dysbindin-1B-HDAC3 complex interfered with the interaction between dysbindin-1 and CRM1, inhibiting the nucleocytoplasmic shuttling of dysbindin-1, in addition to its regulation of synapsin I expression. Further study is required to gain a better understanding of the detailed molecular mechanisms through which the dysbindin-1-HDAC3 complex translocates from the cytoplasm to the nucleus.

Interestingly, we also found that, of the three dysbindin-1 isoforms, HDAC3 phosphorylation increased only in the presence of dysbindin-1B. Since dysbindin-1A and -1B have different C-termini, we hypothesize that C-terminal sequence divergence may be the basis of their isoform-specific interaction properties.

Previous studies suggested that HDAC3 phosphorylation enhances the deacetylase activity of HDAC3 [11,32]. In this study, we demonstrated that the dysbindin-1-HDAC3 complex facilitated HDAC3 phosphorylation, possibly leading to regulation of its deacetylase activity. HDAC3 forms a complex with NCoR and SMRT, and this complex deacetylates histones such as H3 and H4 [13]. HDAC3 complexes also interact with transcription factors and repress transcription [13]. Dysbindin-1 may affect transcription through an interaction with HDAC3.

In conclusion, in this study we provide the first evidence of an interaction between dysbindin-1 and HDAC3 that regulates the subcellular distribution of dysbindin-1 and HDAC3 phosphorylation. Further study is needed to elucidate the influence of dysbindin-1 on the downstream pathway of HDAC3, such as the histone acetylation, possibly providing a novel target for the treatment of schizophrenia.

Acknowledgments

This work was supported by an Intramural Research Grants (23-5) for Neurological and Psychiatric Disorders of NCNP from the Ministry of Health, Labor and Welfare, Japan, and Comprehensive Research on Disability Health and Welfare, the Ministry of Health, Labor and Welfare, Japan (to S.I.).

Appendix A. Supplementary data

Supplementary material related to this article can be found, in the online version, at http://dx.doi.org/10.1016/j.neulet.2014.08.046.

References

[1] S.K. Bhardwaj, M. Baharnoori, B. Sharif-Askari, A. Kamath, S. Williams, L.K. Srivastava, Behavioral characterization of dysbindin-1-deficient sandy mice, Behav. Brain Res. 197 (2009) 435–441.

[2] N.J. Brav, P.R. Buckland, M.J. Owen, M.C. O'Donovan, Cis-acting variation in the expression of a high proportion of genes in human brain, Hum. Genet. 113 (2003) 149–153.

[3] G.C. Carlson, K. Talbot, T.B. Halene, M.J. Gandal, H.A. Kazi, L. Schlosser, Q.H. Phung, R.E. Gur, S.E. Arnold, S.J. Siegel, Dysbindin-1 mutant mice implicate reduced fast-phasic inhibition as a final common disease mechanism in schizophrenia, Proc. Natl. Acad. Sci. U. S. A. 108 (43) (2011) E962–E970.

[4] D.S. Cha, P.A. Kudlow, A. Baskaran, R.B. Mansur, R.S. McIntyre, Implications of epigenetic modulation for novel treatment approaches in patients with schizophrenia, Neuropharmacology 77 (2014) 461–466.

[5] M.M. Cox, A.M. Tucker, J. Tang, K. Talbot, D.C. Richer, L. Yeh, S.E. Arnold, Neurobehavioral abnormalities in the dysbindin-1 mutant, sandy, on a C57BL/6 J genetic background, Genes Brain Behav. 8 (2009) 390–397.

[6] E. Fei, X. Ma, C. Zhu, T. Xue, J. Yan, Y. Xu, J. Zhou, G. Wang, Nucleocytoplasmic shuttling of dysbindin-1, a schizophrenia-related protein, regulates synapsin I expression, J. Biol. Chem. 285 (2010) 38630–38640.

[7] Y.Q. Feng, Z.Y. Zhou, X. He, H. Wang, X.L. Guo, C.J. Hao, Y. Guo, X.C. Zhen, W. Li, Dysbindin deficiency in sandy mice causes reduction of snapin and displays behaviors related to schizophrenia, Schizophr. Res. 106 (2008) 218–228.

[8] D.P. Gavin, S. Kartan, K. Chase, D.R. Grayson, R.P. Sharma, Reduced baseline acetylated histone 3 levels, and a blunted response to HDAC inhibition in lymphocyte cultures from schizophrenia subjects, Schizophr. Res. 103 (2008) 330–332.

[9] S. Hattori, T. Murotani, S. Matsuzaki, T. Ishizuka, N. Kumamoto, M. Takeda, M. Tohyama, A. Yamatodani, H. Kunugi, R. Hashimoto, Behavioral abnormalities and dopamine reductions in sdy mutant mice with a deletion in Dtnbp1, a susceptibility gene for schizophrenia, Biochem. Biophys. Res. Commun. 373 (2008) 298–302.

[10] H. Ito, R. Morishita, T. Shinoda, I. Iwamoto, K. Sudo, K. Okamoto, K. Nagata, Dysbindin-1, WAVE2 and Abi-1 form a complex that regulates dendritic spine formation, Mol. Psychiatry 15 (2010) 976–986.

[11] M. Jeyakumar, X.F. Liu, H. Erdjument-Bromage, P. Tempst, M.K. Bagchi, Phosphorylation of thyroid hormone receptor-associated nuclear receptor corepressor holocomplex by the DNA-dependent protein kinase enhances its histone deacetylase activity, J. Biol. Chem. 282 (2007) 9312–9322.

[12] S.C. McQuown, R.M. Barrett, D.P. Matheos, R.J. Post, G.A. Rogge, T. Alenghat, S.E. Mullican, S. Jones, J.R. Rusche, M.A. Lazar, M.A. Wood, HDAC3 is a critical negative regulator of long-term memory formation, J. Neurosci. 31 (2011) 764–774.

[13] S.C. McQuown, M.A. Wood, HDAC3 and the molecular brake pad hypothesis, Neurobiol. Learn. Mem. 96 (2011) 27–34.

[14] J.K. Millar, J.C. Wilson-Annan, S. Anderson, S. Christie, M.S. Taylor, C.A. Semple, R.S. Devon, D.M. St Clair, W.J. Muir, D.H. Blackwood, D.J. Porteous, Disruption of two novel genes by a translocation co-segregating with schizophrenia, Hum. Mol. Genet. 9 (2000) 1415–1423.

[15] H. Okuda, R. Kuwahara, S. Matsuzaki, S. Miyata, N. Kumamoto, T. Hattori, S. Shimizu, K. Yamada, K. Kawamoto, R. Hashimoto, M. Takeda, T. Katayama, M. Tohyama, Dysbindin regulates the transcriptional level of myristoylated alanine-rich protein kinase C substrate via the interaction with NF-YB in mice brain, PLoS ONE 5 (2010) e8773.

[16] S. Oyama, H. Yamakawa, N. Sasagawa, Y. Hosoi, E. Futai, S. Ishiura, Dysbindin-1, a schizophrenia-related protein, functionally interacts with the DNA-dependent protein kinase complex in an isoform-dependent manner, PLoS ONE 4 (2009) e4199.

[17] S.G. Schwab, M. Albus, J. Hallmayer, S. Hönig, M. Borrmann, D. Lichtermann, R.P. Ebstein, M. Ackenheil, B. Lerer, N. Risch, M. Wolfgang, D.B. Wildenauer, Evaluation of a susceptibility gene for schizophrenia on chromosome 6p by multipoint affected sib-pair linkage analysis, Nat. Genet. 11 (1995) 325–327.

[18] S.C. Schwab, M. Knapp, S. Mondabon, J. Hallmayer, M. Borrmann-Hassenbach, M. Albus, B. Lerer, M. Rietschel, M. Trixler, W. Maier, D.B. Wildenauer, Support for association of schizophrenia with genetic variation in the 6p22.3 gene, dysbindin, in sib-pair families with linkage and in an additional sample of triad families, Am. J. Hum. Genet. 72 (2003) 185–190.

[19] H. Stefansson, E. Sigurdsson, V. Steinthorsdottir, S. Bjornsdottir, T. Sigmundsson, S. Ghosh, J. Brynjolfsson, S. Gunnarsdottir, O. Ivarsson, T.T. Chou, O. Hjaltason, B. Birgisdottir, H. Jonsson, V.G. Gudnadottir, E. Gudmundsdottir, A. Bjornsson, B. Ingvarsson, A. Ingason, S. Sigfusson, H. Hardardottir, R.P. Harvey, D. Lai, M. Zhou, D. Brunner, V. Mutel, A. Gonzalo, G. Lemke, J. Sainz, G. Johannesson, T. Andresson, D. Gudbjartsson, A. Manolescu, M.L. Frigge, M.E. Gurney, A. Kong, J.R. Gulcher, H. Petursson, K. Stefansson, Neuregulin 1 and susceptibility to schizophrenia, Am. J. Hum. Genet. 71 (2002) 877–892.

[20] R.E. Straub, Y. Jiang, C.J. MacLean, Y. Ma, B.T. Webb, M.V. Myakishev, C. Harris-Kerr, B. Wormley, H. Sadek, B. Kadambi, A.J. Cesare, A. Gibberman, X. Wang, F.A. O'Neill, D. Walsh, K.S. Kendler, Genetic variation in the 6p22.3 gene DTNBP1, the human ortholog of the mouse dysbindin gene, is associated with schizophrenia, Am. J. Hum. Genet. 71 (2002) 337–348.

[21] R.E. Straub, C.J. MacLean, F.A. O'Neill, J. Burke, B. Murphy, F. Duke, R. Shinkwin, B.T. Webb, J. Zhang, D. Walsh, K.S. Kendler, A potential vulnerability locus for schizophrenia on chromosome 6p24-22: evidence for genetic heterogeneity, Nat. Genet. 11 (1995) 287–293.

[22] Y. Takami, T. Nakayama, N-terminal region, C-terminal region, nuclear export signal, and deacetylation activity of histone deacetylase-3 are essential for the viability of the DT40 chicken B-cell line, J. Biol. Chem. 275 (2000) 6191–6201.

[23] K. Takao, K. Toyama, K. Nakanishi, S. Hattori, H. Takamura, M. Takeda, T. Miyakawa, R. Hashimoto, Impaired long-term memory retention and working memory in sdy mutant mice with a deletion in Dtnbp1, a susceptibility gene for schizophrenia, Mol. Brain 1 (2008) 11.

[24] K. Talbot, W.L. Eidem, C.L. Tinsley, M.A. Benson, E.W. Thompson, R.J. Smith, C.G. Hahn, S.J. Siegel, J.Q. Trojanowski, R.E. Gur, D.J. Blake, S.E. Arnold, Dysbindin-1 is reduced in intrinsic, glutamatergic terminals of the hippocampal formation in schizophrenia, J. Clin. Invest. 113 (2004) 1353–1363.

[25] K. Talbot, N. Louneva, J.W. Cohen, H. Kazi, D.J. Blake, S.E. Arnold, Synaptic dysbindin-1 reductions in schizophrenia occur in an isoform-specific manner indicating their subsynaptic location, PLoS ONE 6 (2011) e16886.

[26] K. Talbot, W.Y. Ong, D.J. Blake, J. Tang, N. Louneva, G.C. Carlson, S.E. Arnold, Dysbindin-1 and its protein family, in: A. Lajtha, D. Javitt, J. Kantrowitz (Eds.), Handbook of Neurochemistry and Molecular Neurobiology, Springer, Berlin, 2009, pp. 107–241.

[27] B. Tang, B. Dean, E.A. Thomas, Disease- and age-related changes in histone acetylation at gene promoters in psychiatric disorders, Transl. Psychiatry 1 (2011) e64.

[28] S. Wang, C.E. Sun, C.A. Walczak, J.S. Ziegle, B.R. Kipps, L.R. Goldin, S.R. Diehl, Evidence for a susceptibility locus for schizophrenia on chromosome 6pter-p22, Nat. Genet. 10 (1995) 41–46.

[29] C.S. Weickert, D.A. Rothmond, T.M. Hyde, J.E. Kleinman, R.E. Straub, Reduced DTNBP1 (dysbindin-1) mRNA in the hippocampal formation of schizophrenia patients, Schizophr. Res. 98 (2008) 105–110.

[30] C.S. Weickert, R.E. Straub, B.W. McClintock, M. Matsumoto, R. Hashimoto, T.M. Hyde, M.M. Herman, D.R. Weinberger, J.E. Kleinman, Human dysbindin (DTNBP1) gene expression in normal brain and in schizophrenic prefrontal cortex and midbrain, Arch. Gen. Psychiatry 61 (2004) 544–555.

[31] W.M. Yang, S.C. Tsai, Y.D. Wen, G. Fejer, E. Seto, Functional domains of histone deacetylase-3, J. Biol. Chem. 277 (2002) 9447–9454.

[32] X. Zhang, Y. Ozawa, H. Lee, Y.D. Wen, T.H. Tan, B.E. Wadzinski, E. Seto, Histone deacetylase 3 (HDAC3) activity is regulated by interaction with protein serine/threonine phosphatase 4, Genes Dev. 19 (2005) 827–839.

Journal of Neuroscience Research

Journal of Neuroscience Research 92:671–678 (2014)

Nonredundant Function of Two Highly Homologous Octopamine Receptors in Food-Deprivation-Mediated Signaling in *Caenorhabditis elegans*

Midori Yoshida,[1] Eitaro Oami,[2] Min Wang,[3] Shoichi Ishiura,[1,2] and Satoshi Suo[2]*

[1]Department of Biological Sciences, Graduate School of Science, University of Tokyo, Tokyo, Japan
[2]Department of Life Sciences, Graduate School of Arts and Sciences, University of Tokyo, Tokyo, Japan
[3]College of Arts and Sciences, University of Tokyo, Tokyo, Japan

It is common for neurotransmitters to possess multiple receptors that couple to the same intracellular signaling molecules. This study analyzes two highly homologous G-protein-coupled octopamine receptors using the model animal *Caenorhabditis elegans*. In *C. elegans*, the amine neurotransmitter octopamine induces activation of cAMP response element-binding protein (CREB) in the cholinergic SIA neurons in the absence of food through activation of the Gq-coupled octopamine receptor SER-3 in these neurons. We also analyzed another Gq-coupled octopamine receptor, SER-6, that is highly homologous to SER-3. As seen in *ser-3* deletion mutants, octopamine- and food-deprivation-mediated CREB activation was decreased in *ser-6* deletion mutants compared with wild-type animals, suggesting that both SER-3 and SER-6 are required for signal transduction. Cell-specific expression of SER-6 in the SIA neurons was sufficient to restore CREB activation in the *ser-6* mutants, indicating that SER-6, like SER-3, functions in these neurons. Taken together, these results demonstrate that two similar G-protein-coupled receptors, SER-3 and SER-6, function in the same cells in a nonredundant manner.

Key words: G-protein-coupled receptor; CREB; octopamine; *C. elegans*; food deprivation

Amine neurotransmitters, such as dopamine, noradrenaline, and serotonin, signal primarily through G-protein-coupled receptors (GPCRs). Each neurotransmitter is capable of binding multiple receptors, which in turn couple different G proteins, allowing a single neurotransmitter to activate multiple intracellular signaling pathways. In many cases, multiple receptors bind to the same neurotransmitter and activate the same intracellular signaling cascades. The α_1-adrenergic receptors, for example, consist of three subtypes, α_{1a}, α_{1b}, and α_{1d}. All three receptors bind to both adrenaline and noradrenaline, couple to G protein Gq, and induce activation of phospholipase C. The physiological significance of having multiple receptors with the same function is not well understood. Studies in receptor-knockout mice suggest that these receptors may not be entirely redundant, in part because expression of each receptor is restricted to distinct cell types (Chen and Minneman, 2005).

Recent studies have shown that GPCRs are capable of regulating each other through the formation of heterodimers in vivo and in doing so acquire new functions (Gupta et al., 2010; Pei et al., 2010; He et al., 2011). Functionally similar receptors have been shown to form heterodimers when expressed heterologously in cultured cells, suggesting that these types of receptors can work cooperatively. For example, the α_{1b}-adrenergic receptor facilitates internalization of the α_{1a}-adrenergic receptor by forming a hetero-oligomer, without affecting the pharmacology or signaling of either receptor (Stanasila et al., 2003). Similarly, the α_{1b}-adrenergic receptor is capable of binding the α_{1d}-adrenergic receptor, facilitating its expression on the surface of the cell (Hague et al., 2004). This heterodimer behaves as a single functional entity with increased signaling (Hague et al., 2006). Together, these interactions suggest that similar receptors may perform nonredundant functions when expressed in the same cell. This study analyzes two homologous receptors, SER-3 and SER-6, which likely couple to the same G protein signaling in the model organism *Caenorhabditis elegans*.

Amine neurotransmitters regulate activation of cAMP response element-binding protein (CREB) in *C. elegans* (Suo et al., 2006, 2009). CREB is a transcription factor that plays essential roles in a variety of biological

Contract grant sponsor: KAKENHI, Contract grant number: 23115705 (to S.S.); Contract grant number: 23700439 (to S.S.); Contract grant sponsor: Ministry of Health, Labor and Welfare, Japan, Contract grant number: 23-5 (to S.I.).

*Correspondence to: Satoshi Suo, Komaba 3–8–1, Meguro-ku, Tokyo, 153–8902, Japan. E-mail: suo@bio.c.u-tokyo.ac.jp

Received 20 July 2013; Revised 30 October 2013; Accepted 17 November 2013

Published online 21 January 2014 in Wiley Online Library (wileyonlinelibrary.com). DOI: 10.1002/jnr.23345

processes (Lonze and Ginty, 2002; Johannessen et al., 2004). It binds to specific DNA sequences called cAMP response elements (CRE) and regulates expression of its target genes upon phosphorylation (Mayr and Montminy, 2001). Using a reporter for CREB activation, we previously found that CREB is activated in the cholinergic SIA neurons in the absence of food (Suo et al., 2006). This signaling is mediated by the amine neurotransmitter octopamine, which is considered to be the biological equivalent of mammalian noradrenaline (Roeder, 1999), because food-deprivation-mediated CREB activation was decreased in the octopamine-deficient mutant *tbh-1* and CREB can be activated by addition of exogenous octopamine. SER-3, a putative Gq-coupled octopamine receptor, and EGL-30, an α subunit of Gq, function in the SIA neurons to induce CREB activation. Furthermore, this octopamine signaling is suppressed by dopamine through activation of the dopamine receptors DOP-2 and DOP-3 (Suo et al., 2009).

In addition to SER-3, *C. elegans* has another putative octopamine receptor, SER-6, that is highly homologous to SER-3. SER-6 has been shown to bind octopamine and is believed to couple Gq because of its ability to activate inward currents upon octopamine treatment when heterologously expressed in *Xenopus* oocytes, which presumably is mediated by endogenous Ca^{2+}-gated chloride channels (Mills et al., 2012). In this study, we show that SER-6 is involved in octopamine-mediated CREB activation and functions in SIA neurons, similarly to SER-3. Interestingly, loss of either SER-3 or SER-6 leads to diminished signaling, indicating that both receptors are required for normal signaling. These two similar octopamine receptors are therefore working in the same cells and function in a nonredundant manner in vivo.

MATERIALS AND METHODS

Strains

Culturing and genetic manipulation of *C. elegans* were performed as described previously (Brenner, 1974). The alleles used in this study were as follows: *ser-3(ad1774)* I (Suo et al., 2006), *ser-6(tm2104)* IV and *ser-6(tm2146)* IV (gifts from the National BioResource Project [NBRP], Ministry of Education, Culture, Sports, Science and Technology [MEXT], Tokyo, Japan), *octr-1(ok371)X* (Wragg et al., 2007), *tyra-3(ok325)X* (Wragg et al., 2007), *unc-64(e246) III* (Brenner, 1974), *tbh-1(ok1196)* (Suo et al., 2006), and *tzIs3[cre::gfp; lin-15(+)* (Kimura et al., 2002). All mutants used in the CREB activity assay carry *cre::gfp* reporter. These mutants were generated by mating *tzIs3* males with other mutants. The resulting genotypes were confirmed by PCR. *tbh-1(ok1196);tzIs3*, *ser-3(ad1774);tzIs3*, and *unc-64(e246)III;tzIs3* were constructed previously (Suo et al., 2006).

Cloning of *ser-6*

Total *C. elegans* RNA was extracted from all stages of a wild-type Bristol N2 strain using Trizol reagent (Gibco BRL, Rockville, MD). The cDNA of SER-6 was synthesized using a gene-specific primer (5′-TACATACAATTGAATTTCAG-3′) and the Prime Script 1st strand cDNA synthesis kit (TaKaRa). PCR was carried out with a SER-6 reverse primer (5′-GAA CAATTATTACTGAACTGC-3′) and an SL1 primer (5′-GGTTTAATTACCCAAGTTTGAG-3′) matching the 5′-trans-spliced leader sequence found on *C. elegans* RNAs (Blaxter and Liu, 1996) using PfuUltra High-Fidelity DNA Polymerase (Stratagene, La Jolla, CA). The resulting PCR product was cloned into pCR-Blunt (Invitrogen, Carlsbad, CA) and sequenced.

Phylogenetic Analysis

The amino acid sequences of SER-6 and other biogenic amine receptors of human and invertebrates were aligned with ClustalW (DNA Databank of Japan), using relatively well-conserved regions excluding the N terminus, second extracellular loop, third intracellular loop, and the C terminus of these receptors. The phylogenic tree was drawn with PHYLIP by the Fitch-Margoliash method and visualized with TreeView.

Analyses of CRE-Mediated Gene Expression

CREB activation assays were performed as described previously (Suo et al., 2006, 2009). Briefly, animals carrying *cre::gfp* were synchronized by a hypochlorite treatment, and the resulting eggs were placed on NGM plates seeded with *Escherichia coli* OP50 (Brenner, 1974). Animals were incubated for 2 days at 20°C, transferred to new NGM plates, and incubated for an additional 24 hr. Animals were then transferred onto assay plates and incubated for 4 hr at 20°C. Each assay plate contained 1.7% AgarNoble (BD Diagnostics, San Jose, CA) with or without 3 mg/ml octopamine-hydrochloride (Sigma-Aldrich, St. Louis, MO), with bacterial food spread on its surface. For food-depletion assays, synchronized animals were incubated on NGM plates seeded with or without OP50 at 20°C for 6 hr. For soaking assays, synchronized animals were incubated for 4 hr at 20°C on 60-mm NGM plates seeded with bacterial food and overlaid with ~5 ml water. After incubation, animals were collected in M9 buffer (Brenner, 1974) containing 50 mM NaN_3 and mounted on glass slides. The number of SIA neurons expressing green fluorescent protein (GFP) was counted for each animal using a fluorescence microscope (Olympus BX53) to quantify CREB activation. All counting was performed by an experimenter blinded to the genotype and incubation conditions of the animals. Statistical significance was evaluated by an analysis of variance followed by a Tukey-Kramer multiple-comparisons test in GraphPad Prism. Images of animals were obtained with the fluorescence microscope.

Analyses of *ser-6* Expression Patterns

The transcriptional reporter fusion gene *ser-6::gfp* was generated using the fusion PCR method as described elsewhere (Hobert, 2002) using the primers Y54fusionA (5′-GTTAA GCTCCTCGAACTTTCGG-3′), Y54fusionB (5′-AGTCGA CCTGCAGGCATGCAAGCTGCCCAGCGTCAGTGATA GC-3′), Y54fusionE (5′-CTCTCAAACTTTCCGGCGC-3′), fusionD (5′-AAGGGCCCGTACGGCCGACTAGTAGG-3′), fusionF (5′-GGAAACAGTTATGTTTGGTATATTGGG-3′), and fusionC (5′-AGCTTGCATGCCTGCAGGTCGACT-3′). The region corresponding to 5.0-kb upstream and a part of

exon 1 of *ser-6* gene was amplified with the primers Y54fusionA and Y54fusionB by LA Taq (TaKaRa) using genomic DNA as the template. The resulting PCR product was fused to 2–1876 of pPD95.75. *ser-6::gfp* was injected into N2 wild-type animals together with *ceh-17::dsred* (Pujol et al., 2000; Suo et al., 2006), *tbh-1::dsred* (Alkema et al., 2005; Suo et al., 2006), pBluescript (Stratagene), and the transformation marker pRF4, which contains the dominant roller mutation *rol-6(su1006)* (Kramer et al., 1990), as described by Mello et al. (1991). Concentrations of the injected plasmids were 30, 10, 10, 30, and 20 ng/μl, respectively. Images of transformants were obtained with a confocal laser microscope (Leica inverted microscope DMI6000 B).

Cell-Specific Rescue of *ser-6*

To express *ser-6* in the SIA neurons, cDNA of *ser-6* was fused to the *ceh-17* promoter, which induces gene expression in only the SIA and ALA neurons. The coding sequence of *ser-6* was amplified with the corresponding forward (5′-TTCGCC ACCGGTAAAAATGATTTTGCTATC-3′) and reverse (5′-AAATAAGCGGCCGCTCAAAATTTTGGCTTC-3′) primers by PfuUltra High-Fidelity DNA Polymerase (Stratagene) using subcloned *ser-6* cDNA as the template. The PCR product was digested with the restriction enzymes *Age*I and *Not*I and cloned into *Age*I- and *Not*I-digested *ceh-17::dop-2l* (Suo et al., 2009) to obtain *ceh-17::ser-6*. *ceh-17::ser-6* was then injected into *ser-6(tm2104);tzIs3* together with the transformation marker *lin-44::gfp* (Murakami et al., 2001) and pBluescript (Stratagene). The concentrations of the injected *ceh-17::ser-6*, *lin-44::gfp*, and pBluescript were 10, 20, and 70 ng/μl, respectively. Animals carrying *lin-44::gfp*, reflected by expression of GFP in the tail hypodermis, were analyzed in the rescue experiments.

Generation of Heterozygous Mutants and Overexpression of *ser-3* and *ser-6*

To generate heterozygous mutant animals, *ser-3(ad1774);ser-6(tm2104);tzIs3* males, *unc-64(e246)III;tzIs3* hermaphrodites, *ser-3(ad1774);unc-64(e246)III;tzIs3* hermaphrodites, or *ser-6(tm2104);unc-64(e246)III;tzIs3* hermaphrodites were mated before each assay. *unc-64* homozygous animals exhibit an uncoordinated phenotype (Unc; Brenner, 1974). Only non-Unc F1 animals were tested, because Unc animals result from self-fertilization.

To obtain strains that overexpress SER-6 in the SIA neurons, *ceh-17::ser-6* was injected into *ser-3(ad1774);tzIs3*, together with *lin-44::gfp* and pBluescript (Stratagene). The concentrations of the injected expression plasmids, *lin-44::gfp*, and pBluescript were 10, 10, and 80 ng/μl, respectively. CREB activation was analyzed using transformants that express GFP in the tail hypodermis.

To obtain strains that overexpress SER-3 in the SIA neurons, the *ceh-17::ser-3* fusion construct (Suo et al., 2006) was injected into *ser-3(ad1774);tzIs3* together with *lin-44::gfp* and pBluescript (Stratagene). The concentrations of the injected expression plasmids, *lin-44::gfp*, and pBluescript were 10, 10, and 80 ng/μl, respectively. The transformant was then mated with *tzIs3* males, and the sibling *tzIs3* animals carrying the *ceh-17::ser-3* fusion construct were mated with *ser-6(tm2104);tzIs3* males to obtain *ser-6(tm2104);tzIs3* carrying the *ceh-17::ser-3* fusion gene.

RESULTS

SER-6 Is Highly Homologous to the Gq-Coupled Octopamine Receptor SER-3

SER-6 was identified as an amine neurotransmitter receptor by comparing the amino acid sequences of amine receptors between human and *C. elegans* (Chase et al., 2004). Srinivasan et al. (2008) showed that *ser-6* deletion mutants have a defect in serotonin-induced reduction of fat storage. Furthermore, Mills et al. (2012) showed that SER-6 is required for octopamine-mediated alteration of octanol sensitivity. SER-6 has also been shown to function as an octopamine receptor and possibly couple to the Gq signal pathway by an electrophysiological experiment using *Xenopus* oocyte heterologously expressing SER-6 (Mills et al., 2012).

We cloned cDNA of *ser-6* and compared the amino acid sequence of SER-6 with that of SER-3 (Fig. 1A,B). SER-3 is likely a Gq-coupled octopamine receptor and increases intracellular Ca^{2+} concentration in response to 10 nM octopamine when expressed in HEK293 cells (Petrascheck et al., 2007). As expected, SER-3 and SER-6 were highly homologous. The phylogenic tree including human and invertebrate amine receptors (Fig. 1C) shows that SER-6 is homologous to other Gq-coupled octopamine receptors of invertebrates, including SER-3 and insect octopamine receptors AmOAMB and DmOAMB (Han et al., 1998; Grohmann et al., 2003). Among mammalian amine receptors, SER-6 was most closely related to the human α_1-adrenergic receptors, which are also Gq-coupled receptors.

SER-6 Is Involved in Octopamine-Dependent CREB Activation in the SIA Neurons

In *C. elegans*, CREB activation can be detected by fluorescence in animals carrying a *cre::gfp* reporter, in which CRE is fused to a GFP sequence (Kimura et al., 2002). Using this reporter, we have shown that food deprivation induces CREB activation in the SIA neurons (Suo et al., 2006, 2009). This response appears to be mediated through octopamine, because exogenously applied octopamine similarly activates CREB in the SIA neurons, and mutants in the *tbh-1* gene, which encodes a tyramine β-hydroxylase required for octopamine synthesis (Alkema et al., 2005), exhibit decreased response to food deprivation. SER-3 has been shown to function in the SIA neurons to transmit octopamine signaling through EGL-30, the α subunit of Gq. Here, we determined whether SER-6 is also involved in this CREB activation.

Animals carrying *cre::gfp* were exposed to 3 mg/ml octopamine for 4 hr or deprived of food for 6 hr. The number of SIA neurons in each animal expressing GFP was then counted to quantify CREB activation. Wild-type animals exhibited significant GFP expression in the SIA neurons following octopamine treatment or food deprivation (Fig. 2B,E). *C. elegans* has four SIA neurons

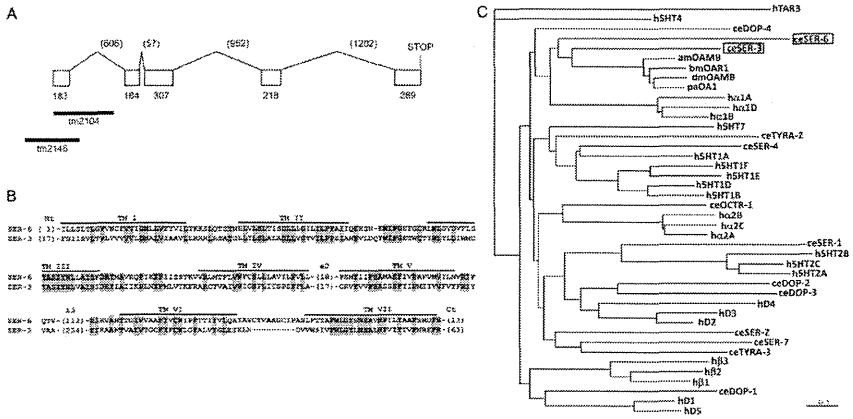

Fig. 1. Gene structure of *ser-6* and comparison between SER-6 and other amine receptors. *ser-6* cDNA was cloned, and the structure of this gene was identified. Black bars indicate the region deleted in the *tm2104* and *tm2146* alleles (**A**). The amino acid sequence of SER-6 was aligned with SER-3 (**B**). Predicted transmembrane (TMs) regions are overscored. Amino acid residues conserved between SER-6 and SER-3 are indicated by gray shading. Numbers in parentheses represent the number of amino acids not shown in the figure. According to the phylogenic tree of SER-6 and other biogenic amine receptors of human and invertebrates, SER-3 and SER-6 are highly homologous (**C**). The amino acid sequences of each receptor were aligned with ClustalW using relatively conserved regions, excluding the N terminus, second extracellular loop, third intracellular loop, and C terminus. The phylogenic tree was calculated by using the PHYLIP package and the Fitch-Margoliash method. Receptor sequences used and the GenBank accession numbers are as follows: *C. elegans* octopamine receptors (ceSER-3, NP491954; ceOCTR-1, CCD83472.1), *C. elegans* dopamine receptors (ceDOP-1, CCD68411.1; ceDOP-2, CBY85347.1; ceDOP-3, NP_001024907.2l ceDOP-4, CCD65696.1), *C. elegans* tyramine receptors (ceTYRA-2, CCD83463.1; ceTYRA-3, CCD83479.1; ceSER-2, NP_001024335.1), *C. elegans* serotonin receptors (ceSER-1, CCD63419.1; ceSER-4, CCD73768.1; ceSER-7, CCD83456.1), insect α-adrenergic-like octopamine receptors (dmOAMB, AAC17442; amOAMB, CAD67999; paOA1, AAP93817.1; bmOAR1, NP_001091748.1), human dopamine receptors (hD1, P21728; hD2, P14416; hD3, P35462; hD4, P21917; hD5, P21918), human serotonin receptors (h5HT1a, I38209; h5HT1b, JN0268; h5HT1d, A53279; h5HT1e, A45260; h5HT1f, A47321; h5HT2a, A43956; h5HT2b, S43687; h5HT2c, JS0616; h5HT4, Q13639; h5HT7, A48881), and human adrenergic receptors (hα1A, NP000671; hα1B, NP000670; hα1D, NP000669; hα2A, A34169; hα2B, A37223; hα2C, A31237; hβ1, QRHUB1; hβ2, QRHUB2; hβ3, QRHUB3). A human trace amine receptor 3 (hTAR3, AAO24660) was used as an out group. bm, *Bombyx mori*; pa, *Periplaneta americana*; dm, *Drosophila melanogaster*; am, *Apis mellifera*.

(SIADL, SIADR, SIAVL, and SIAVR) and there was no apparent difference in GFP expression rates of these four neurons. As reported previously, this CRE-mediated gene expression was dependent on SER-3, with *ser-3* mutants showing decreased responses to exogenous octopamine and food deprivation (Fig. 2F). Next, we examined two deletion alleles of *ser-6*, *tm2104* and *tm2146*, and found that octopamine-mediated GFP expression was decreased in both mutants (Fig. 2D,G,H). These results suggest that SER-6 is also required for octopamine-dependent CREB activation in the SIA neurons. CREB activation levels induced by food deprivation were also decreased in *ser-6* animals (Fig. 2G,H), suggesting that SER-6 is involved in food deprivation-induced CREB activation in the SIA neurons.

The response to food deprivation was significantly attenuated in octopamine-deficient *tbh-1* mutants (Fig. 2J). However, a small response was observed, consistent with previous reports (Suo et al., 2006), suggesting that the response to food deprivation is partially octopamine independent. The level of CREB activation observed in the *ser-3* mutants in the absence of food was similar to that of *tbh-1*. We also analyzed *tbh-1;ser-3* double mutants and found that *tbh-1;ser-3* responded to food deprivation slightly more strongly than *ser-3* and *tbh-1* single mutants (Fig. 2K). The reason for this increase is unknown. However, because CREB activation was not decreased by the *tbh-1* mutation in the double mutants, it is likely that the CREB activity observed in the *ser-3* mutants is octopamine independent. In contrast, the level of CREB activation in the *ser-6* mutants was higher than that in the *tbh-1* mutants, and the level of CREB activation in the *tbh-1;ser-6* mutants was similar to that in the *tbh-1* mutants (Fig. 2L). These results suggest that some octopamine-dependent signaling is occurring in the absence of *ser-6*. These experiments were repeated in *ser-3;ser-6* double mutants, and their responses to exogenous octopamine and food deprivation were similar to those of the *ser-3* mutants (Fig. 2I).

CREB is activated in the SIA neurons when animals are soaked in water, and this soaking response is independent of octopamine (Suo et al., 2006). *ser-6* mutants responded normally to soaking (Fig. 2G), exhibiting robust activation of CREB. This result confirms that the SIA neurons are present in *ser-6* mutants and that CREB can be activated in these neurons under certain conditions. Reduced octopamine-mediated CREB activation seen in the *ser-6* mutants is therefore not the result of abnormal development of SIA neurons.

In addition to SER-3 and SER-6, the *C. elegans* genome contains another octopamine receptor, OCTR-

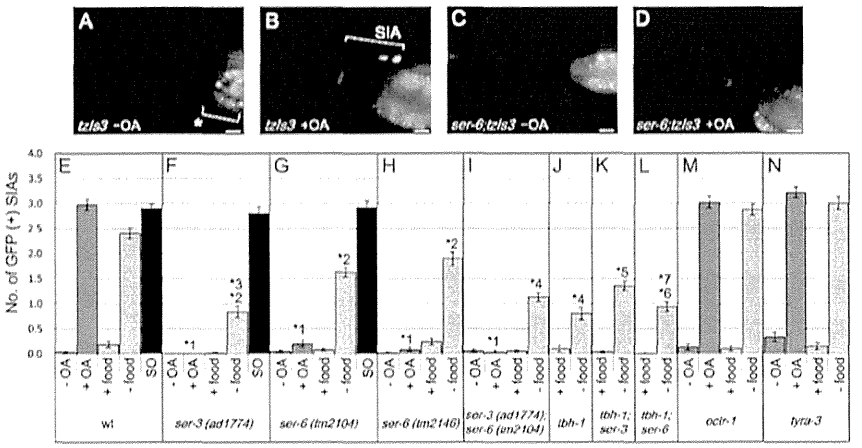

Fig. 2. Octopamine- and food deprivation-induced CREB activation in the SIA neurons. Animals carrying *cre::gfp* were cultured on agar plates containing 0 (**A,C**) or 3 mg/ml (**B, D**) octopamine. Fluorescent images were obtained from wild-type background animals (A,B) and *ser-6(tm2104)* mutants (C,D) after 4 hr of incubation. GFP expression was induced by exogenous octopamine in the SIA neurons of wild-type but not *ser-6* mutants. The bracket marked with an asterisk indicates autofluorescence of the intestine. Wild-type, *ser-3(ad1774)*, *ser-6(tm2104)*, *ser-6(tm2146)*, *ser-3(ad1774);ser-6(tm2104)*, *tbh-1(ok1196)*, *tbh-1(ok1196);ser-3(ad1774)*, *tbh-1(ok1196);ser-6(tm2104)*, *octr-1(ok371)*, and *tyra-3(ok325)* mutants carrying *cre::gfp* were incubated on plates containing 0 or 3 mg/ml octopamine (OA) for 4 hr, incubated on NGM plates with or without food for 6 hr, or soaked in water (SO) in the presence of food for 4 hr. The number of GFP-expressing SIA neurons per animal was then determined (**E–N**). Error bars indicate the standard errors of the mean. At least 53 animals were tested. *1$P < 0.001$ (Tukey–Kramer multiple-comparisons test) compared with +OA of wild-type animals. *2$P < 0.001$ compared with −food of wild-type animals. *3$P < 0.001$ compared with −food of *ser-6(tm2104)* mutants. *4$P > 0.05$ compared with −food of *ser-3* mutants. *5$P < 0.001$ compared with −food of *tbh-1* mutants and *ser-3* mutants. *6$P > 0.05$ compared with −food of *tbh-1* mutants. *7$P < 0.001$ compared with −food of *ser-6(tm2104)* mutants. Scale bars = 10 μm. [Color figure can be viewed in the online issue, which is available at wileyonlinelibrary.com.]

1, as well as the tyramine receptor TYRA-3, which has been shown to bind octopamine, albeit weakly (Wragg et al., 2007). We therefore investigated whether OCTR-1 and TYRA-3 are involved in octopamine-mediated CREB activation. The *octr-1* and *tyra-3* mutants responded normally to exogenous octopamine and food deprivation, suggesting that these receptors are not involved in the octopamine-mediated CREB activation seen in the SIA neurons (Fig. 2M,N).

SER-6 Functions in the SIA Neurons to Activate CREB

The observation that octopamine-induced CREB activation was reduced in both *ser-3* and *ser-6* single mutants indicates that both SER-3 and SER-6 are required for CREB activation. Furthermore, the observation that the response to food deprivation in *ser-3;ser-6* double mutants was not smaller than that of either *ser-3* or *ser-6* single mutants also suggests that SER-3 and SER-6 are not redundant. One possibility is that they function in different neurons. Notably, it has been shown that both SER-3 and SER-6 are required for regulation of octanol sensitivity by octopamine and that they function in different neurons for this regulation (Mills et al., 2012). Another possibility is that SER-3 and SER-6 function in the same (SIA) neurons and there may be some interaction at the molecular level. It has been previously reported that ser-6 is expressed in a subset of head and tail neurons (Srinivasan et al., 2008). However, it has not been determined whether *ser-6* is expressed in the SIA neurons. We generated a *ser-6::gfp* reporter fusion gene in which 5 kb of upstream sequence plus a portion of exon 1 are fused to the *gfp* gene. This fusion gene was coinjected along with the *ceh-17::dsred* reporter. The *ceh-17* promoter was used because it induces gene expression in only the four SIA neurons and one additional neuron (the ALA neuron; Pujol et al., 2000). The *ceh-17::dsred* reporter therefore labels the SIA neurons with DsRed expression. A *tbh-1::dsred* reporter construct was also introduced to label the octopaminergic RIC neurons. In these transformants, GFP expression was observed in multiple neurons, with GFP colocalizing with DsRed (Fig. 3), suggesting that *ser-6* is expressed in both the SIA and the RIC neurons.

To determine whether SER-6 functions in the SIA neurons, we performed a cell-specific rescue experiment. We introduced the *ceh-17::ser-6* fusion construct, in which the *ceh-17* promoter was fused to SER-6 cDNA, into *ser-6(tm2104)* mutant animals. These transformants should express SER-6 in only the SIA and ALA neurons. As shown in Figure 4, the transgenic animals responded to exogenous octopamine as robustly as did the wild-type animals, suggesting that expression of SER-6 in the SIA neurons is sufficient to restore CREB activation upon octopamine. CREB activation of the transformants in response to food deprivation was not significantly different from that of the wild-type animals, also suggesting that SER-6 functions in the SIA neurons for food-deprivation response. However, there was no significant difference between CREB activation levels for food deprivation of

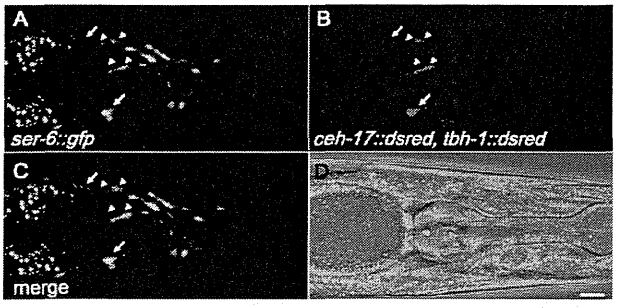

Fig. 3. Expression pattern of *ser-6*. Fluorescent (**A–C**) and corresponding differential interference contrast (**D**) images were obtained from N2 animals carrying the *ser-6::gfp*, *ceh-17::dsred*, and *tbh-1::dsred* constructs. The SIA- and RIC-neuron-specific promoters, *ceh-17* and *tbh-1*, respectively, were used to label the SIA and RIC neurons with DsRed. Merged images show the colocalization of GFP and DsRed. Arrowheads indicate SIA neurons. Arrows indicate RIC neurons. Scale bar = 10 μm. [Color figure can be viewed in the online issue, which is available at wileyonlinelibrary.com.]

ser-6 animals and the transformants. Therefore, it remains possible that *ser-6* also functions in other cells.

Both SER-3 and SER-6 Are Required for Normal CREB Activation in SIA Neurons

The present results suggest that SER-3 and SER-6 function in the same cells and that both of these receptors are required for normal signaling, despite having similar functions. One explanation for the decreased CREB activation seen in *ser-3* and *ser-6* single mutants is a decrease in the total number of octopamine receptors. A specific level of octopamine receptor may be required for normal signaling, and removal of either of these two genes results in an insufficient quantity of octopamine receptors. To address this possibility, we assayed CREB activation in double heterozygous *ser-3/+;ser-6/+* animals. The double heterozygous animals responded slightly more weakly to exogenous octopamine treatment than wild-type animals (Fig. 5B). However, the response of the double heterozygous animals was much stronger than that of the *ser-3* or *ser-6* single mutants, which was essentially zero (Figs. 2F–H, 5B). This result suggests that having both *ser-3* and *ser-6* is important for CREB activation rather than the quantity of octopamine receptor genes. The response to food deprivation was not different between *ser-3/+;ser-6/+* double heterozygous animals and wild-type animals (Fig. 5A,B). Furthermore, we analyzed the *ser-3/ser-3;ser-6/+* and *ser-3/+;ser-6/ser-6* heterozygous animals and found that *ser-3/ser-3;ser-6/+* were similar to *ser-3* single mutants ($P > 0.05$; Figs. 2F, 5C) and that *ser-3/+;ser-6/ser-6* were similar to *ser-6* single mutants ($P > 0.05$; Figs. 2G, 5D) with respect to their response to food deprivation. These results suggest that removing one copy of the *ser-3* or *ser-6* gene has little effect on the response to food deprivation, which further supports the idea that normal CREB activation requires the existence of both octopamine receptors rather than just a specific quantity of receptor.

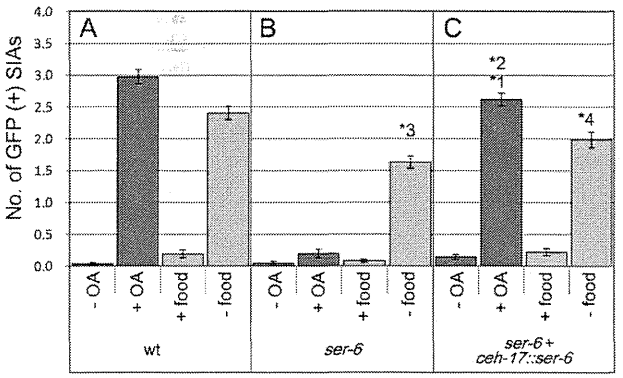

Fig. 4. SIA-neuron-specific rescue of the *ser-6* CREB activation phenotype. The transgenes *ceh-17::ser-6 and lin-44::gfp* were introduced into a *ser-6(tm2104)* mutant carrying *cre::gfp*. The *ceh-17* promoter induces gene expression in only the SIA and ALA neurons. The *lin-44::gfp* construct was used as a cotransformation marker. Transformants were incubated on plates containing 0 or 3 mg/ml octopamine for 4 hr or on NGM plates with or without food for 6 hr (**C**). At least 72 animals were tested. Error bars indicate the standard errors of the mean. CREB activity in wild-type animals and *ser-6(tm2104)* mutants shown in Figure 2E,G is reprinted (**A,B**). $*1P < 0.001$ (Tukey–Kramer multiple-comparisons test) compared with +OA of *ser-6* mutants. $*2P > 0.05$ compared with +OA of wild-type animals. $*3P < 0.001$ compared with −food of wild-type animals. $*4P > 0.05$ compared with −food of wild-type animals.

To address the effect of the gene dosage further, we next assessed CREB activation in animals overexpressing either SER-3 or SER-6. SER-3 was overexpressed in the SIA neurons of the *ser-6* deletion mutant using the *ceh-17::ser-3* fusion construct, and SER-6 was overexpressed in the SIA neurons of *ser-3* deletion mutant using the *ceh-17::ser-6* fusion construct. These animals therefore lacked either SER-6 or SER-3 but overexpressed the other receptor in the SIA neurons, in addition to endogenous expression. It has been shown that multiple copies (typically over 100 copies) of genes are retained in transgenic animals when transformed by injection (Fire et al., 1991). In *ser-3* mutants overexpressing SER-6, CREB activation induced by exogenous octopamine or food deprivation was similar to that for *ser-3* deletion mutants alone ($P > 0.05$; Figs. 2F, 5E). This result suggests that SER-6 alone cannot induce activation of CREB, even when SER-6 is overexpressed. In *ser-6* mutants overexpressing SER-3, some spontaneous CREB activation was observed on the control plates that did not contain octopamine but did contain food (Fig. 5F, first bar). However, this activation was not seen on NGM plates containing food (Fig. 5F, third bar); the cause of this difference is unknown. One possible explanation is that, because control plates for octopamine treatment contained less salts and peptone than NGM plates, these compounds, or the difference in the condition of the bacteria growing on these plates, might have affected CREB activation in this strain. Nonetheless, a moderate increase in CREB activation was observed upon exogenous octopamine treatment in the *ser-3*-overexpressing animals (Fig. 5F), suggesting that SER-3 can partially respond to exogenous

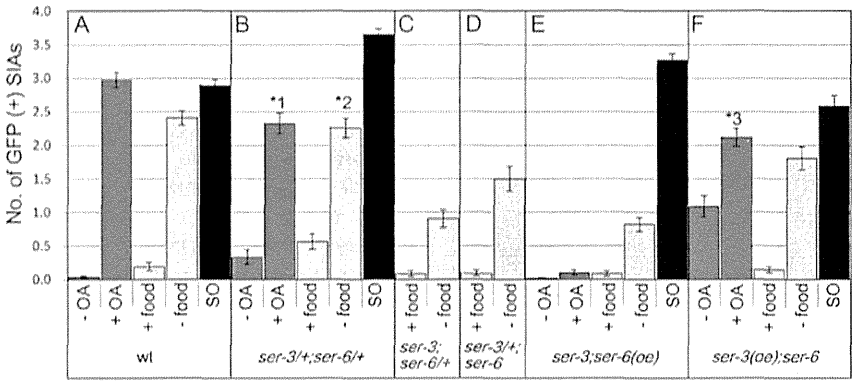

Fig. 5. Octopamine- and food deprivation-mediated CREB activity in heterozygous and overexpressing animals. Double heterozygous animals (**B**), *ser-3/ser-3;ser-6/+* animals (**C**), *ser-3/+;ser-6/ser-6* animals (**D**), *ser-6*-overexpressing animals (E), and *ser-3*-overexpressing animals (F) carrying *cre::gfp* were incubated on plates containing 0 or 3 mg/ml octopamine for 4 hr, incubated on NGM plates with or without food for 6 hr, or soaked in water (SO) in the presence of food for 4 hr. The number of GFP-expressing SIA neurons per animal was then determined. At least 43 animals were tested. Error bars indicate standard errors of the mean. CREB activity in wild-type animals shown in Figure 2E is reprinted (**A**). $*1P < 0.01$ (Tukey–Kramer multiple-comparisons test) compared with +OA of wild-type animals. $*2P > 0.05$ compared with −food of wild-type animals. $*3P < 0.001$ compared with -OA of *ser-3(oe);ser-6* animals.

octopamine without SER-6 when overexpressed. In contrast, the level of CREB activation induced by food deprivation in *ser-3*-overexpressing animals was not different from that of *ser-6* mutants ($P > 0.05$). Collectively, these results suggest that both *ser-3* and *ser-6* are required for full activation of CREB regardless of their quantity and that *ser-3* but not *ser-6* can partially function by itself only when it is overexpressed.

DISCUSSION

It is common for neurotransmitters to possess multiple receptors that couple to the same intracellular signaling. When expressed in a heterologous system, such functionally similar receptors function in a nonredundant manner through receptor–receptor interactions. This study analyzed two homologous octopamine receptors of *C. elegans*, SER-3 and SER-6, which have been shown to couple to the same class of G proteins (Petrascheck et al., 2007; Mills et al., 2012). These receptors were both required for octopamine-mediated CREB activation in the SIA neurons. Cell-specific rescue experiments revealed that SER-6, like SER-3, functions in the SIA neurons, indicating that these receptors function in the same cells. These results suggest that SER-3 and SER-6 act together to transmit octopamine signaling in the SIA neurons.

Using SER-3- and SER-6-overexpressing animals, we further demonstrated that both SER-3 and SER-6 are required for normal CREB activation by octopamine; overexpression of one receptor in the absence of the other could not fully restore normal CREB activation. *ser-3*-overexpressing animals did respond to exogenous octopamine in the absence of *ser-6*, although the response was much weaker than that in the wild-type animals. In contrast, SER-6 could not activate CREB without SER-3 even when overexpressed. These results indicate that, when overexpressed, SER-3 can partially bypass the requirement for SER-6. In addition, CREB activation by food deprivation was stronger in *ser-6* mutants than in *ser-3* mutants or *ser-3;ser-6* double mutants (Fig. 2), suggesting that SER-3 can also partially activate CREB without SER-6 in this condition. One possible mechanism in which SER-3 and SER-6 function cooperatively is that SER-6 functions in part to assist the function of SER-3 by controlling the quantity of functional SER-3. Another possibility is that SER-3 and SER-6 form a dimer and that the heterodimer transmits stronger signals than monomers or homodimers. It has been shown that structurally similar GPCRs can form heterodimers and that dimerization affects their membrane expression as well as their signaling strength (Stanasila et al., 2003; Hague et al., 2004, 2006). It also remains possible that, even though SER-3 and SER-6 are structurally similar, they transmit different intracellular signals in vivo and these signals converge to activate CREB fully. Further efforts, including expression of SER-3 and SER-6 in a heterologous expression system, would be required to elucidate the precise mechanisms by which these receptors function cooperatively.

We found that SER-3 and SER-6 are coexpressed in the SIA neurons. Although both SER-3 and SER-6 are also expressed in other neurons, the expression patterns of these receptors overlap only partially. Neurons expressing only SER-3 or SER-6 are unlikely to be able to respond to octopamine stimulation by fully activating CREB, unlike the SIA neurons. It therefore is possible that, by utilizing multiple functionally similar receptors differentially expressed across several cells types, the nervous system diversifies its sensitivity to neurotransmitters, allowing for more complex neuronal regulation.

ACKNOWLEDGMENTS

We thank Drs. Yuichi Iino and Masahiro Tomioka (University of Tokyo) for their help with confocal

microscopy. *ser-6* Mutants were provided by the National BioResource Project, Ministry of Education, Culture, Sports, Science and Technology. Some strains were provided by the CGC, which is funded by the NIH Office of Research Infrastructure Programs (P40 OD010440).

REFERENCES

Alkema MJ, Hunter-Ensor M, Ringstad N, Horvitz HR. 2005. Tyramine Functions independently of octopamine in the *Caenorhabditis elegans* nervous system. Neuron 46:247–260.

Blaxter M, Liu L. 1996. Nematode spliced leaders—ubiquity, evolution and utility. Int J Parasitol 26:1025–1033.

Brenner S. 1974. The genetics of *Caenorhabditis elegans*. Genetics 77:71–94.

Chase DL, Pepper JS, Koelle MR. 2004. Mechanism of extrasynaptic dopamine signaling in *Caenorhabditis elegans*. Nat Neurosci 7:1096–1103.

Chen ZJ, Minneman KP. 2005. Recent progress in α1-adrenergic receptor research. Acta Pharmacol Sin 26:1281–1287.

Fire A, Albertson D, Harrison SW, Moerman DG. 1991. Production of antisense RNA leads to effective and specific inhibition of gene expression in *C. elegans* muscle. Development 113:503–514.

Grohmann L, Blenau W, Erber J, Ebert PR, Strunker T, Baumann A. 2003. Molecular and functional characterization of an octopamine receptor from honeybee (*Apis mellifera*) brain. J Neurochem 86:725–735.

Gupta A, Mulder J, Gomes I, Rozenfeld R, Bushlin I, Ong E, Lim M, Maillet E, Junek M, Cahill CM, Harkany T, Devi LA. 2010. Increased abundance of opioid receptor heteromers after chronic morphine administration. Sci Signaling 3:ra54.

Hague C, Uberti MA, Chen Z, Hall RA, Minneman KP. 2004. Cell surface expression of $\alpha 1_d$-adrenergic receptors is controlled by heterodimerization with $\alpha 1_b$-adrenergic receptors. J Biol Chem 279:15541–15549.

Hague C, Lee SE, Chen Z, Prinster SC, Hall RA, Minneman KP. 2006. Heterodimers of $\alpha 1_b$- and $\alpha 1_d$-adrenergic receptors form a single functional entity. Mol Pharmacol 69:45–55.

Han KA, Millar NS, Davis RL. 1998. A novel octopamine receptor with preferential expression in *Drosophila* mushroom bodies. J Neurosci 18:3650–3658.

He SQ, Zhang ZN, Guan JS, Liu HR, Zhao B, Wang HB, Li Q, Yang H, Luo J, Li ZY, Wang Q, Lu YJ, Bao L, Zhang X. 2011. Facilitation of μ-opioid receptor activity by preventing δ-opioid receptor-mediated codegradation. Neuron 69:120–131.

Hobert O. 2002. PCR fusion-based approach to create reporter gene constructs for expression analysis in transgenic *C. elegans*. Biotechniques 32:728–730.

Johannessen M, Delghandi MP, Moens U. 2004. What turns CREB on? Cell Signal 16:1211–1227.

Kimura Y, Corcoran EE, Eto K, Gengyo-Ando K, Muramatsu MA, Kobayashi R, Freedman JH, Mitani S, Hagiwara M, Means AR, Tokumitsu H. 2002. A CaMK cascade activates CRE-mediated transcription in neurons of *Caenorhabditis elegans*. EMBO Rep 3:962–966.

Kramer JM, French RP, Park EC, Johnson JJ. 1990. The *Caenorhabditis elegans rol-6* gene, which interacts with the *sqt-1* collagen gene to determine organismal morphology, encodes a collagen. Mol Cell Biol 10:2081–2089.

Lonze BE, Ginty DD. 2002. Function and regulation of CREB family transcription factors in the nervous system. Neuron 35:605–623.

Mayr B, Montminy M. 2001. Transcriptional regulation by the phosphorylation-dependent factor CREB. Nat Rev Mol Cell Biol 2:599–609.

Mello CC, Kramer JM, Stinchcomb D, Ambros V. 1991. Efficient gene transfer in *C. elegans*: extrachromosomal maintenance and integration of transforming sequences. EMBO J 10:3959–3970.

Mills H, Wragg R, Hapiak V, Castelletto M, Zahratka J, Harris G, Summers P, Korchnak A, Law W, Bamber B, Komuniecki R. 2012. Monoamines and neuropeptides interact to inhibit aversive behaviour in *Caenorhabditis elegans*. EMBO J 31:667–678.

Murakami M, Koga M, Ohshima Y. 2001. DAF-7/TGF-β expression required for the normal larval development in *C. elegans* is controlled by a presumed guanylyl cyclase DAF-11. Mech Dev 109:27–35.

Pei L, Li S, Wang M, Diwan M, Anisman H, Fletcher PJ, Nobrega JN, Liu F. 2010. Uncoupling the dopamine D1-D2 receptor complex exerts antidepressant-like effects. Nat Med 16:1393–1395.

Petrascheck M, Ye X, Buck LB. 2007. An antidepressant that extends lifespan in adult *Caenorhabditis elegans*. Nature 450:553–556.

Pujol N, Torregrossa P, Ewbank JJ, Brunet JF. 2000. The homeodomain protein CePHOX2/CEH-17 controls antero-posterior axonal growth in *C. elegans*. Development 127:3361–3371.

Roeder T. 1999. Octopamine in invertebrates. Prog Neurobiol 59:533–561.

Srinivasan S, Sadegh L, Elle IC, Christensen AG, Faergeman NJ, Ashrafi K. 2008. Serotonin regulates *C. elegans* fat and feeding through independent molecular mechanisms. Cell Metab 7:533–544.

Stanasila L, Perez JB, Vogel H, Cotecchia S. 2003. Oligomerization of the $\alpha 1_a$- and $\alpha 1_b$-adrenergic receptor subtypes. Potential implications in receptor internalization. J Biol Chem 278:40239–40251.

Suo S, Kimura Y, Van Tol HH. 2006. Starvation induces cAMP response element-binding protein-dependent gene expression through octopamine-Gq signaling in *Caenorhabditis elegans*. J Neurosci 26:10082–10090.

Suo S, Culotti JG, Van Tol HH. 2009. Dopamine counteracts octopamine signalling in a neural circuit mediating food response in *C. elegans*. EMBO J 28:2437–2448.

Wragg RT, Hapiak V, Miller SB, Harris GP, Gray J, Komuniecki PR, Komuniecki RW. 2007. Tyramine and octopamine independently inhibit serotonin-stimulated aversive behaviors in *Caenorhabditis elegans* through two novel amine receptors. J Neurosci 27:13402–13412.

Genes to Cells

ABLIM1 splicing is abnormal in skeletal muscle of patients with DM1 and regulated by MBNL, CELF and PTBP1

Natsumi Ohsawa[1], Michinori Koebis[1], Hiroaki Mitsuhashi[1], Ichizo Nishino[2] and Shoichi Ishiura[1]*

[1]*Department of Life Sciences, Graduate School of Arts and Sciences, The University of Tokyo, 3-8-1, Komaba, Meguro-ku, Tokyo 153-8902, Japan*
[2]*National Institute of Neuroscience, National Center of Neurology and Psychiatry (NCNP), 4-1-1 Ogawahigashi, Kodaira, Tokyo 187-8502, Japan*

Myotonic dystrophy type 1 (DM1) is an RNA-mediated disorder characterized by muscle weakness, cardiac defects and multiple symptoms and is caused by expanded CTG repeats within the 3′ untranslated region of the *DMPK* gene. In this study, we found abnormal splicing of actin-binding LIM protein 1 (*ABLIM1*) in skeletal muscles of patients with DM1 and a DM1 mouse model (HSA^{LR}). An exon 11 inclusion isoform is expressed in skeletal muscle and heart of non-DM1 individuals, but not in skeletal muscle of patients with DM1 or other adult human tissues. Moreover, we determined that *ABLIM1* splicing is regulated by several splice factors, including MBNL family proteins, CELF1, 2 and 6, and PTBP1, using a cellular splicing assay. MBNL proteins promoted the inclusion of *ABLIM1* exon 11, but other proteins and expanded CUG repeats repressed exon 11 of *ABLIM1*. This result is consistent with the hypothesis that MBNL proteins are trapped by expanded CUG repeats and inactivated in DM1 and that CELF1 is activated in DM1. However, activation of PTBP1 has not been reported in DM1. Our results suggest that the exon 11 inclusion isoform of *ABLIM1* may have a muscle-specific function, and its abnormal splicing could be related to muscle symptoms of DM1.

Introduction

Myotonic dystrophy (dystrophia myotonica, DM) is an autosomal dominant disorder and is the most common form of muscular dystrophy that affects adults. Characteristic symptoms of DM include muscle hyperexcitability (myotonia), progressive muscle atrophy, muscle weakness, cataracts, defects in cardiac conduction, cognitive impairment and insulin resistance (Harper 2001). There are two forms of DM, DM1 and DM2, which are caused by expansion of a CTG repeat in the 3′ untranslated region (3′-UTR) of DM protein kinase (*DMPK*) and a CCTG repeat in intron 1 of CCHC-type zinc finger and nucleic acid binding protein (*CNBP/ZNF9*), respectively (Brook *et al.* 1992; Mahadevan *et al.* 1992; Fu *et al.* 1993; Liquori *et al.* 2001). Accumulating evidence suggests that transcribed RNA CUG or CCUG repeats may be the cause of several symptoms and cellular abnormality in patients with DM. First, the number of CUG repeats correlates with symptom severity in DM1 (Mahadevan *et al.* 1992). Second, nuclear accumulation of expanded CUG and CCUG repeats in RNA is observed in cells derived from patients with DM1 and DM2, respectively (Taneja *et al.* 1995; Davis *et al.* 1997; Liquori *et al.* 2001). Third, HSA^{LR} transgenic mice, which express an expanded CUG repeat RNA inserted into the 3′-UTR of the *human skeletal muscle actin* (*HSA*) gene, manifest myotonia and abnormal muscle histology (Mankodi *et al.* 2000). Therefore, understanding the pathomechanism of DM is important to determine how expanded repeat RNAs perturb normal cellular function.

Abnormalities of alternative splicing have been found in cells from patients with DM and some DM mice models. Abnormal splicing has been reported in several genes, such as chloride channel 1 (*CLCN1*; Charlet *et al.* 2002b; Mankodi *et al.* 2002), troponin T type 2 (cardiac) (*TNNT2/cTNT*; Philips *et al.*

Communicated by: Yoshikazu Nakamura
**Correspondence:* cishiura@mail.ecc.u-tokyo.ac.jp

DOI: 10.1111/gtc.12201

1998), bridging integrator 1 (*BIN1*; Fugier *et al.* 2011), ATPase, Ca^{2+} transporting, cardiac muscle, fast twitch 1 (*ATP2A1*; Kimura *et al.* 2005), L-type Ca^{2+} channel and voltage sensor (*Cav1.1*; Tang *et al.* 2012), insulin receptor (*INSR*; Savkur *et al.* 2001) and microtubule-associated protein tau (*MAPT*; Sergeant *et al.* 2001), as well as others. Among them, it was shown that abnormal alternative splicing of *CLCN1*, *BIN1* and *INSR* caused myotonia, muscle weakness and insulin resistance, respectively. These aberrant splicings are caused by an imbalance of two RNA-binding protein families, muscleblind-like splicing regulator (MBNL), and CUGBP and the Elav-like family member (CELF). It has been shown that the functions of MBNL proteins are disrupted in cells of patients with DM because MBNL proteins are sequestered by expanded repeat RNAs within nuclei. MBNL1, MBNL2 and MBNL3 proteins were colocalized with both CUG and CCUG repeat RNA foci (Fardaei *et al.* 2002). In addition, it has been shown that MBNL1 binds directly to CUG and CCUG repeat RNAs in a length-dependent manner *in vitro* (Miller *et al.* 2000; Kino *et al.* 2004). Moreover, MBNL knockout mice, $Mbnl1^{\Delta 3/\Delta 3}$ (Kanadia *et al.* 2003) and $Mbnl2^{-/-}$ (Hao *et al.* 2008), showed abnormal splicing of many genes, as seen in patients with DM and HSA^{LR} mice, and manifested some DM-like symptoms, such as myotonia, abnormal muscle histology and cataracts. However, CELF1 protein expression is elevated in the muscle of patients with DM and DM mouse models in which CELF1 is stabilized by PKC-mediated phosphorylation (Savkur *et al.* 2001; Timchenko *et al.* 2001; Kuyumcu-Martinez *et al.* 2007). In addition, phosphorylation of CELF1 is altered by activation of GSK3β signaling in DM (Salisbury *et al.* 2008; Jones *et al.* 2012). However, the mechanism of PKC and GSK3β activation by expanded repeat RNAs remains unclear. In addition, CELF1 over-expression in mice (MDAFrtTA/TRE-CUGBP1 mice: CELF1 is over-expressed in skeletal muscle by feeding doxycycline-containing food; Ward *et al.* 2010) caused abnormal splicing of several genes and manifested some DM-like symptoms, such as muscle atrophy, weakness and abnormal muscle histology. Importantly, cellular studies have showed that alternative splicing of *CLCN1*, *TNNT2*, *BIN1*, *ATP2A1* and *INSR* is regulated directly by MBNL and/or CELF proteins in an antagonistic manner (Ho *et al.* 2004; Dansithong *et al.* 2005; Hino *et al.* 2007; Kino *et al.* 2009; Fugier *et al.* 2011). Apart from MBNL and CELF, it has been reported that polypyrimidine tract binding protein 1 (PTBP1) and its homologues regulate alternative splicing of many exons that are spliced in a neuron- or muscle-specific manner, such as c-src N1 (Chan & Black 1997), α-actinin SM (Southby *et al.* 1999), α-tropomyosin exon 2 (Gooding *et al.* 1998), NMDAR1 exon 5 (Zhang *et al.* 1999) and *TNNT2* exon 5 (Philips *et al.* 1998; Charlet *et al.* 2002a). Moreover, Ptbp1 expression is repressed during differentiation in neurons (Boutz *et al.* 2007a; Makeyev *et al.* 2007) and C2C12 myoblast (Boutz *et al.* 2007b; Bland *et al.* 2010), and during maturation of heart after birth (Zhang *et al.* 2009). Also, an RNA-binding protein, fox-1 homologue (*Caenorhabditis elegans*) 1 (RBFOX1/FOX1) is mainly expressed in muscle, heart and neurons, and it regulates tissue-specific splicing (Jin *et al.* 2003). In addition, it has been shown that Fox1 expression is up-regulated during differentiation of neuroblastoma and myoblast (Underwood *et al.* 2005). Therefore, it has been thought that the reduction of PTBP1 and the increase of FOX1 are involved in differentiation of neuron or muscle, or in maturation of muscle and heart.

Previously, we attempted to identify novel missplicing events that could be associated with DM muscle symptoms. To determine the splicing abnormality and gene expression resulting from expanded CUG repeat RNAs, we carried out exon arrays using muscle biopsies of patients with DM1. More than 100 splicing events were altered in DM1 muscles and identified aberrant splicing of myomesin 1 (*MYOM1*), PDZ and LIM protein 3 (*PDLIM3*), and fibronectin 1 (*FN1*) (Koebis *et al.* 2010; Ohsawa *et al.* 2010). In this study, we report the abnormal splicing of exon 11 of *actin-binding LIM protein 1* (*ABLIM1*) in skeletal muscle of patients with DM1 and HSA^{LR} mice. The inclusion isoform of *ABLIM1* exon 11 (ex11+) was expressed specifically in normal adult heart and skeletal muscle, but not in other tissues. ABLIM1 protein is expressed mainly in the retina, brain and muscle and is localized to the Z-disk of cardiac muscle (Roof *et al.* 1997). As Z-disks are essential for force transmission, muscle integrity and a nodal point of signaling toward the nucleus (Frey *et al.* 2004; Frank *et al.* 2006), abnormal *ABLIM1* splicing may contribute to the symptoms of DM1.

Results

Aberrant splicing of the ABLIM1 gene in DM1 muscle

To identify aberrant alternative splicing in DM1, we analyzed splicing profiles using an exon array in

biopsies of non-DM individuals (control) and patients with DM1 (Koebis *et al.* 2010). The results suggest that alternative splicing of *ABLIM1* (NC_000010.10) exon 4 and exon 11 is misregulated in DM1 (Fig. S1 in Supporting Information). To verify these results, we carried out reverse transcription polymerase chain reaction (RT-PCR) for *ABLIM1* using biopsies from non-DM individuals and patients with DM1 (Table S1 in Supporting Information). We found that an inclusion of *ABLIM1* exon 11 (ex11+) is suppressed in DM1 muscles (Fig. 1A–C; $P = 0.020$). However, the change in *ABLIM1* exon 4 was not confirmed (Fig. S2 in Supporting Information). As a positive control, we also analyzed the splicing of *ATP2A1* exon 22, which is known to undergo abnormal splicing in patients with DM1 (Kimura *et al.* 2005), and the inclusion of exon 22 was suppressed in DM1 muscles (Fig. S2 in Supporting Information; $P = 0.022$). We investigated whether the ratio of the two isoforms (ex11+ or ex11−) shifts during development of skeletal muscle by RT-PCR (Fig. 1D,E). If a shift is identified, *ABLIM1* splicing might be regulated by factors that change during development. In addition, the alteration in physiological properties of ABLIM1 might be related to DM1 pathogenesis. Only *ABLIM1* ex11− was predominantly expressed in fetal skeletal muscle (fetus: 20 weeks), whereas *ABLIM1* ex11+ was predominantly expressed in skeletal muscle after birth (cont.: 4 years old). In brain and liver, *ABLIM1* ex11− was predominantly expressed, and no *ABLIM1* ex11+ was detected in either fetus or adult tissues. The change in *ABLIM1* splicing was specific to skeletal muscle. ABLIM1 splicing is of the fetal type in DM1, and it is believed that the condition of DM1 muscle appears to be the same as those of fetal muscle. (Fig. 1E) shows the changes in *ABLIM1* splicing in skeletal muscle at several stages: fetus, 8 months, 4 years and 31 years. The change gradually occurred after birth, and *ABLIM1* ex11+ drastically increased between 8 months and 4 years. We also examined the *ABLIM1* splicing pattern in several human tissues (Fig. 1F). *ABLIM1* ex11+ was detected in heart and skeletal muscle; this suggests that *ABLIM1* splicing is regulated in a cardiac and skeletal muscle-specific manner. The expression level was higher in heart than in skeletal muscle.

MBNL, CELF and PTBP1 proteins regulate ABLIM1 exon 11 splicing

To examine whether the MBNL family and CELF family of proteins regulate *ABLIM1* exon 11 splicing, we investigated endogenous *ABLIM1* splicing in human embryonic kidney (HEK) 293 cells transfected with a splicing factor (Fig. 2A). The expression of those splicing factors was confirmed by Western blotting using anti-Myc antibody. Anti-Actin was used as an internal control (Fig. 2B). The inclusion of *ABLIM1* exon 11 was increased by over-expression of MBNL family proteins (two isoforms of MBNL1, EXP40 and EXP42 were used). The CELF family did not change the splicing pattern of endogenous *ABLIM1* in HEK293 cells. We also evaluated the over-expression of MBNL family members in mouse myoblast (C2C12) and human neuroblastoma (SH-SY5Y) cells, but we did not detect any exon 11 inclusion in these cell lines (data not shown) probably because the efficiency of transfection is likely low. In the same assay, *ATP2A1* exon 22 splicing was regulated by all three MBNL proteins (Fig. S3 in Supporting Information). To explore splicing factors that promote *ABLIM1* exon 11 exclusion, we created a minigene containing human *ABLIM1* exons 10, 11 and 12 (Fig. 3A). Our minigene construct does not include internal regions of introns 10 and 11, because, in general, these regions have little influence on splicing (Cooper 2005), and the introns are too long to make the minigene construct. The *ABLIM1* minigene and splicing factor constructs were cotransfected into C2C12 cells, and the splicing pattern of the *ABLIM1* minigene was examined (Fig. 3B). The expression of those splicing factors was confirmed by Western blotting using anti-Myc antibody. Anti-Actin was used as internal control (Fig. 3C). The expression of FOX1 construct was confirmed by real-time PCR (Fig. S4 in Supporting Information) because it was not detected by Western blotting for unknown reasons. FOX1 protein might be cleaved at the front of Myc-tag, or the conformation of Myc-tagged FOX1 might be difficult to detect by Western blotting.

All MBNL proteins and FOX1 up-regulated exon 11 inclusion. In contrast, CELF1, 2 and 6, and PTBP1 down-regulated exon 11 inclusion. It is reported that the expression of Mbnl and Fox1 increases during C2C12 differentiation, whereas those of Celf1 and Ptbp1 decrease. (Bland *et al.* 2010). The exon 11 inclusion was almost undetectable in PTBP1-expressing cells, as seen in DM1 muscles. Thus, we investigated PTBP1 expression levels in patients with DM1 by quantitative RT-PCR. However, its expression did not change significantly in skeletal muscle of patients with DM1 compared to the control (Fig. S5 in Supporting Information).

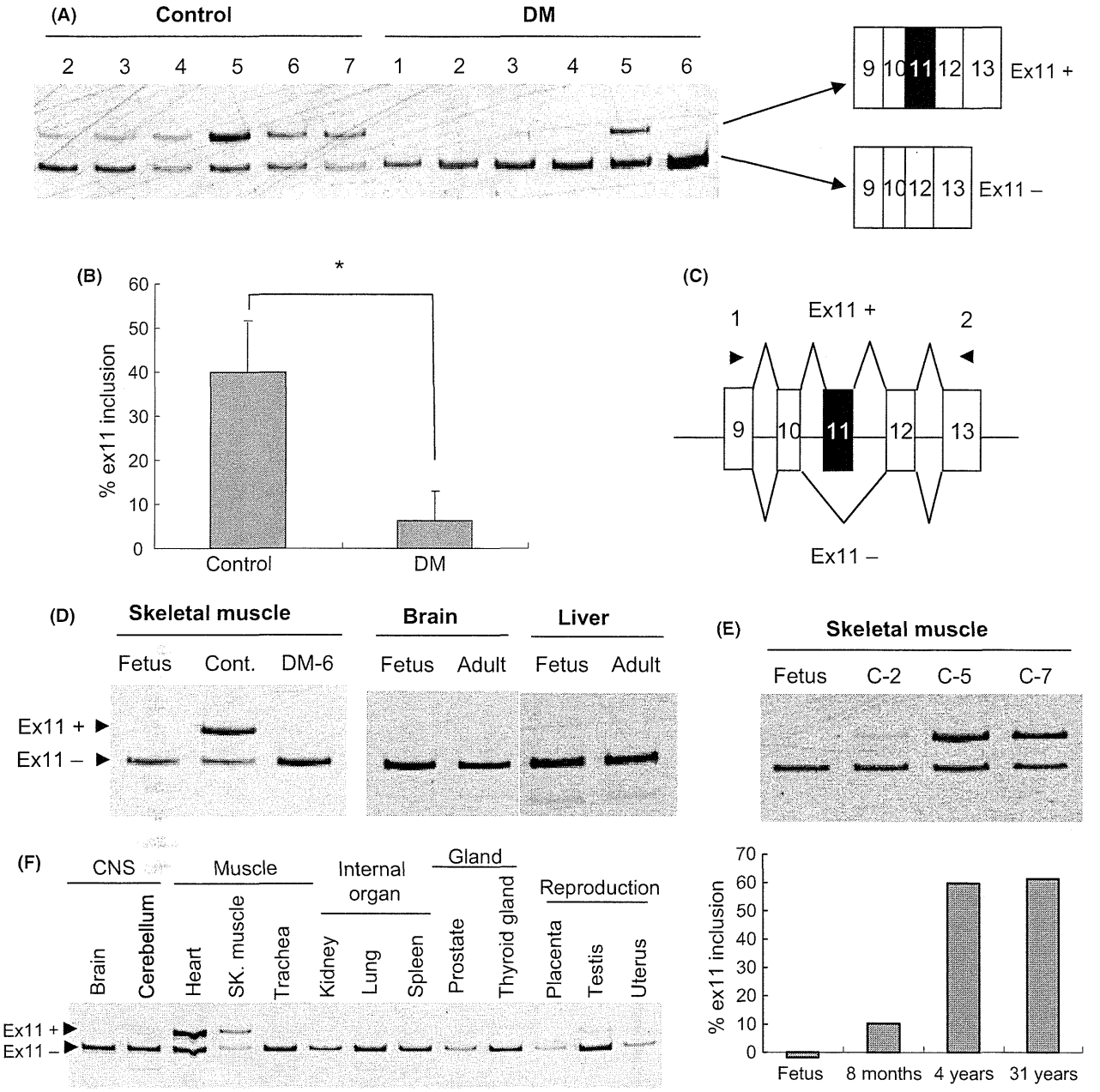

Figure 1 Aberrant *ABLIM1* splicing in patients with DM1. (A) *ABLIM1* ex11+ (exon 11 inclusion isoform) is decreased in DM1. RT-PCR of endogenous *ABLIM1* from DM1 skeletal muscles (n = 6; 1, 2, 3, 4, 5, 6) and non-DM1 muscles as control (n = 6; 2, 3, 4, 5, 6, 7) (B) Percentages of exon 11 inclusion relative to the total transcripts are represented [means ± standard deviation (SD)]. Statistical significance was determined by Student's t-test (*$P < 0.05$). (C) A part of the exon–intron structure of *ABLIM1* and a primer set, we used for RT-PCR (arrowheads 1 and 2). (D) The *ABLIM1* ex11+ (exon 11 inclusion isoform) is a dominant isoform in adult skeletal muscle. On the other hand, ex11− (exon 11 exclusion isoform) is predominant in DM1 and fetal skeletal muscle, and other tissues from the fetus and adult. The change in isoforms from the fetus to adult in skeletal muscle of non-DM does not occur in brain or liver. (E) *ABLIM1* isoform changes from fetus to adult in skeletal muscle. Ex11+ is increased gradually after birth. (F) Endogenous *ABLIM1* splicing in various human tissues. *ABLIM1* ex11+ is detected specifically in heart and skeletal muscle. *ABLIM1* ex11− is expressed ubiquitously in other tissues.

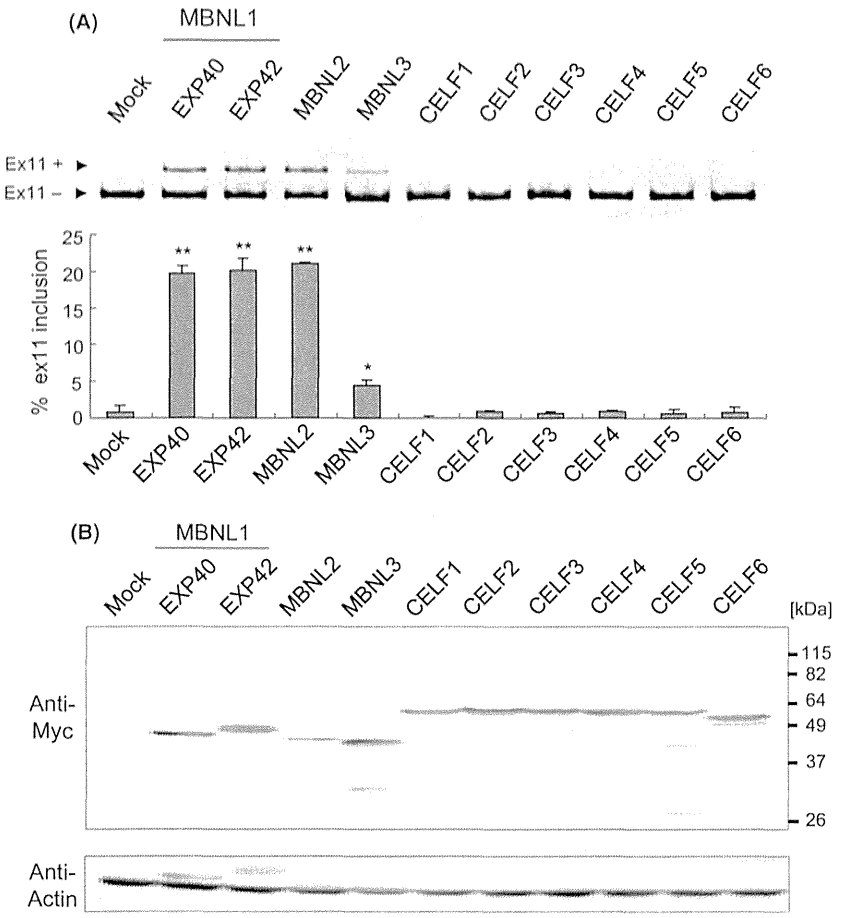

Figure 2 Endogenous *ABLIM1* splicing in HEK293 cells is regulated by MBNL family proteins. (A) EXP40 and EXP42 are spliced isoforms of MBNL1. EXP42 includes exon 6 of the *MBNL1* gene, but EXP40 does not. Splicing factor constructs were transfected into HEK293 cells, and *ABLIM1* exon 11 inclusion was analyzed by RT-PCR shows the percentage of exon 11 inclusion relative to the total transcripts [means ± standard error of the mean (SEM), $n = 3$]. Statistical significance was evaluated by analysis of variance (ANOVA) and Dunnett's multiple comparison tests ($*P < 0.05$, $**P < 0.01$). (B) The lower figure shows the expression of splicing factor proteins detected by Western blotting using anti-Myc antibody. Anti-Actin was used as an internal control.

Next, we carried out knockdown experiments by RNA interference (RNAi) using siRNA to examine whether regulation of *ABLIM1* splicing depends on the dose of endogenous Mbnl1, Celf1, Celf2 or Ptbp1 in mouse C2C12 myoblasts. We tested two or three different siRNAs targeting each mouse Mbnl1, Celf1, Celf2 or Ptbp1. The knockdown efficiency of siMBNL1 (No. 82), siCELF1 (No. 16), siCelf2 (No. 11), siCelf2 (No. 12), siPtbp1 (No. 37), siPtbp1 (No. 38) was especially high (Fig. S6 in Supporting Information), so those siRNAs and two control siRNAs (Medium GC and Low GC) as negative control were used for *ABLIM1* minigene splicing assay (Fig. 3D). siMBNL1 (No. 82) and siCELF1 (No. 16) are siRNAs designed for human MBNL1 and CELF1, but the homologies of the target sequences of the siRNAs are high between human and mouse (96%; 24 bases/25 bases), and it seems that there is no nonspecific targets in mouse genome according to the BLAST search (NCBI). Therefore, we used siMBNL1 (No. 82) and siCELF1 (No. 16) for C2C12 experiments. *ABLIM1* minigene splicing assay showed that siMBNL1 (No. 82) repressed exon 11 inclusion compared to control siRNAs (Cont. Med and Low; Fig. 3D). In contrast, siCelf2 (No. 11), siPtbp1 (No. 37) and siPtbp1 (No. 38) promoted exon 11 inclusion, but siCELF1 (No. 16) and siCelf2 (No. 12) did not alter exon 11 splicing (Fig. 3D). These results suggest that splicing of *ABLIM1* minigene exon 11 is regulated by endogenous Mbnl1 and

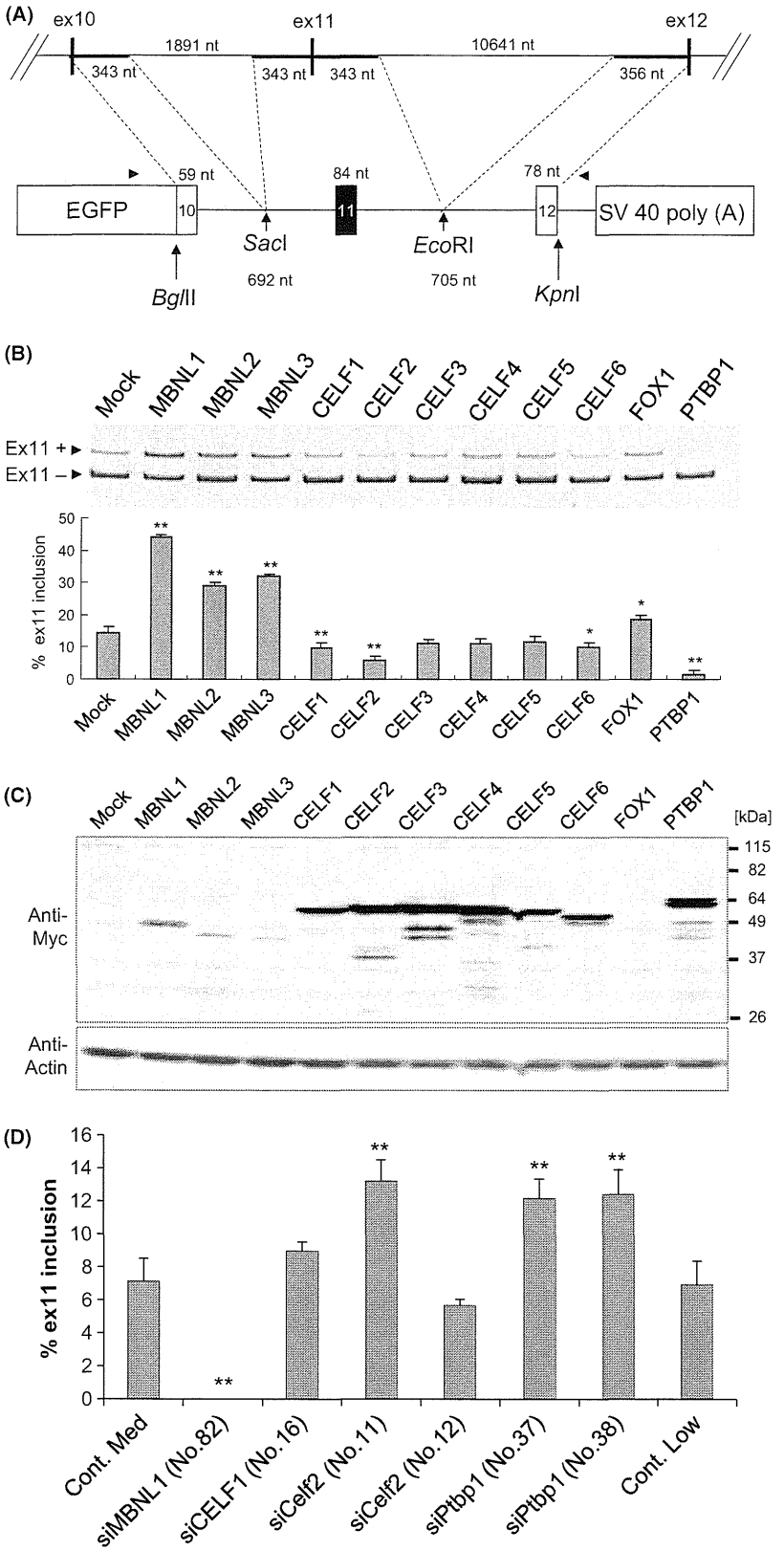

Figure 3 *ABLIM1* minigene splicing is regulated by the MBNL family, CELF family, FOX1 and PTBP1 in C2C12 cells. (A) Design of the *ABLIM1* ex11 minigene, which contains the exon–intron sequence from exon 10 to exon 12. Internal introns 10 and 11 were excluded. Arrowheads indicate primer positions for RT-PCR. (B) The MBNL family, CELF1, 2 and 6, FOX1 and PTBP1 regulate *ABLIM1* minigene splicing in C2C12 cells. The *ABLIM1* minigene (0.3 μg) and mock control or the splice factor vector (1.3 μg) were transfected into C2C12 cells. The lower panel shows the percentage of exon 11 inclusion relative to the total transcripts (means ± SEM, $n = 3$). Statistical significance was assessed by ANOVA and Dunnett's multiple comparison test ($*P < 0.05$, $**P < 0.01$). (C) The upper figure shows the expression of splicing factor constructs by Western blotting using anti-Myc antibody. Anti-Actin was used as an internal control. (D) *ABLIM1* minigene splicing was affected by knockdown of endogenous Mbnl1, Celf2 and Ptbp1, but not Celf1 in C2C12 cells. The *ABLIM1* minigene (0.6 μg) and control duplex RNAs (Cont. Med and Cont. Low) or duplex RNAs against the splicing factors (48 pmol) were transfected into C2C12 cells on 12-well plates. The bar graph shows the percentage of exon 11 inclusion (means ± SEM, $n = 3$) and results of determination of statistical significance ($**P < 0.01$).

Ptbp1, but not Celf1. Endogenous Celf2 may regulate splicing of *ABLIM1* minigene.

CELF family, PTBP1 and expanded CUG repeats antagonize MBNL1 in the regulation of ABLIM1 splicing

To determine whether CELF and PTBP1 can antagonize the effect of MBNL1, CELF1, 2 and 6, and PTBP1 were cotransfected with MBNL1, as well as the *ABLIM1* minigene. The expression of those splicing factors was confirmed by Western blotting using anti-His antibody (Fig. S7 in Supporting Information). As shown in (Fig. 4A), CELF1 (lanes 3, 4), CELF2 (lanes 5, 6), CELF6 (lanes 7, 8) and PTBP1 (lanes 9, 10) decreased the ratio of exon 11 inclusion in a dose-dependent manner. CELF2 and PTBP1 antagonized MBNL1 more strongly than did CELF1 or CELF6. Therefore, we carried out the same assay using a lower dose of CELF2 and PTBP1 (Fig. 4B), and a dose-dependent effect was observed. These results show that CELF1, 2 and 6, and PTBP1 are involved in regulation of *ABLIM1* exon 11 splicing by antagonizing MBNL1. We also investigated the effect of DMPK constructs harboring 0 CTG repeats (DM0), 18 CTG repeats (DM18) or 480 interrupted CTG repeats (DM480) in the 3′-UTR. DM480 repressed exon 11 inclusion more strongly than DM0 and DM18 (Fig. 5). The result suggests that aberrant *ABLIM1* splicing in patients with DM1 is caused by expanded CUG repeats, not caused by the secondary effects. To determine whether expanded CUG repeats can antagonize the effect of MBNL1, DMPK constructs were cotransfected with MBNL1, as well as the *ABLIM1* minigene. DM480 significantly suppressed exon 11 inclusion promoted by MBNL1 compared to DM0 and DM18 (Fig. 5). These results suggest that expanded CUG repeat RNAs antagonize the effect of MBNL1 on *ABLIM1* splicing, most likely due to sequestration of MBNL1 in the expanded CUG repeat RNAs.

Aberrant Ablim1 splicing in a DM mouse model

To further confirm that expanded CTG repeats affect *ABLIM1* splicing *in vivo*, we examined transgenic mice (HSA^{LR}) carrying 250 CTG repeats in the 3′-UTR of the *HSA* gene (Mankodi *et al.* 2000). The *ABLIM1* gene structure differs markedly between mice and humans (Fig. 6A, right). Exon 11 of mouse *Ablim1* is homologous to exon 11 of human *ABLIM1*. RT-PCR analysis showed that both exon 11 and exon 12 of mouse *Ablim1* are alternatively spliced, producing three isoforms, *Ablim1*-I (exon 11 and exon 12 inclusions), *Ablim1*-II (exon 11 inclusion) and *Ablim1*-III (exons 11 and 12 exclusion) in wild-type mice. The inclusion of exon 11 (isoforms I and II) was predominant in wild-type mice (FVB), whereas these isoforms were rare in skeletal muscle of HSA^{LR} mice (Fig. 6A, left). The abnormality was similar to that exhibited by one of the patients with DM. We also examined *Ablim1* splicing in C2C12 during muscle cell differentiation (Fig. 6B). *Ablim1*-III was expressed in undifferentiated myoblasts (d0), whereas *Ablim1*-I and *Ablim1*-II were gradually detected during differentiation (from days 2 to 12). These results indicate that the expression of expanded CTG repeat RNAs is the cause of aberrant splicing of *ABLIM1*, thus inhibiting the inclusion of mature muscle-specific exons.

Discussion

We identified aberrant splicing of *ABLIM1* exon 11 in the skeletal muscle of patients with DM1. Recently, it was reported that *ABLIM1* splicing is abnormal in the heart of patients with DM1 (Kosheleev *et al.* 2010). *ABLIM1* ex11+ (exon 11 inclusion